Received: 4 June 2023 | Revised: 17 October 2023 | Accepted: 12 November 2023
DOI: 10.1111/bre.12833

RESEARCH ARTICLE

Basin Research IAS EAGE WILEY

Facies analysis and sequence stratigraphy of shallow marine, coarse-grained siliciclastic deposits in the southern Utsira High: The Late Jurassic intra-Draupne Formation sandstones in the Johan Sverdrup Field (Norwegian North Sea)

Josep M. Puig López[1] | Miquel Poyatos-Moré[2] | John Howell[1]

[1]Department of Geology and Petroleum Geology, Aberdeen University, Aberdeen, UK
[2]Departament de Geologia, Universitat Autònoma de Barcelona, Cerdanyola del Vallès, Spain

Correspondence
Josep M. Puig López, Department of Geology and Petroleum Geology, Aberdeen University, Aberdeen AB24 3UE, UK.
Email: j.puiglopez.19@abdn.ac.uk

Funding information
Norwegian Research Council

Abstract

Thin, condensed coarse-grained shallow marine successions can be difficult to describe and interpret, especially in the subsurface since the recognition of finer-grained intervals, typically associated with sequence stratigraphic surfaces, is challenging. This lack of mudstones and siltstones means that they also typically make excellent reservoir intervals. The Oxfordian to Volgian intra-Draupne Formation sandstones in the Johan Sverdrup Field, southern Utsira High, represent such a system. This study presents a new sequence stratigraphic model for the Johan Sverdrup Field that unravels the detailed depositional history of the succession and places its formation within a regional Late Jurassic tectonostratigraphic framework. The intra-Draupne Formation sandstones comprise four parasequences deposited following a regional Kimmeridgian marine flooding event. Sediments were mainly supplied through West-derived fan deltas from the Haugaland High and NW-SE-directed tidal currents reworking the Augvald Graben and the Avaldsnes High at the East. The oldest parasequence shows a distinctive suite of facies consisting of fine-grained and mud-rich bioturbated sandstones deposited in a semi-restricted lagoon. Subsequent parasequences lack fine-grained sediments and are dominated by bidirectional cross-stratified, very coarse-to coarse-grained sandstones and gravels deposited in a tidal strait. A progressive reduction of fault-related subsidence in the Middle Volgian along with Late Volgian-Ryazanian sea-level rise and inversion of pre-existing structures promoted backstepping of the feeder systems, sediment starvation and the progressive deposition of the black and green-red shales of the Draupne and Asgard formations. The results of this study account for features previously unidentified in the Johan Sverdrup Field and which have implications for understanding the deposition of coarse-grained shallow marine successions around the Utsira High and other transgressed basement highs.

KEYWORDS

coarse-grained, high, Jurassic, lagoon, marine, parasequence, strait, tidal

1 | INTRODUCTION

The Late Jurassic period in the North Sea was one of the most important time intervals for the accumulation of source and reservoir rocks (Cornford, 1998; Gautier, 2005). A period of rift-related structural reconfiguration and marine incursions promoted the development of a variety of shallow-to-deep marine sedimentary environments strongly influenced by inherited and syn-rift palaeotopograhy: tide-dominated deltas and coastal spits of the Sognefjord Formation (Dreyer et al., 2005), storm-influenced shorefaces of the Fulmar and Ula formations (Baniak et al., 2014; Howell et al., 1996; Johnson et al., 1986), shelf sand ridges of the Rogn Formation (Chiarella et al., 2020) and fan deltas, fault-block submarine fans and channels of the intra-Draupne Formation sandstones (Henstra et al., 2023; Jackson & Larsen, 2008; Jackson et al., 2012; Nøttvedt et al., 2000; Partington et al., 1993). The intra-Draupne Formation sandstones, in this case study, are part of an Oxfordian to Volgian marine clastic package (158 to 147 Ma old, approximately) present throughout the Norwegian North Sea which typically occurs close to the margins of fault blocks, structural highs and major landmasses (Henstra et al., 2023; Tillmans et al., 2021). In 2010, the intra-Draupne Formation sandstones were discovered on the Utsira High, a long-term basement high located in the South Viking Graben giving rise to the Johan Sverdrup Field, one of the largest hydrocarbon discoveries made in the Norwegian Continental Shelf (NCS) (Ottesen et al., 2022; Rønnevik et al., 2017). The intra-Draupne Formation sandstones in the Johan Sverdrup Field were deposited in a shallow marine environment, with grain sizes ranging mostly from pebbles to coarse sandstones and virtually no fine-grained component (Olsen et al., 2017; Ottesen et al., 2022). These types of successions are relatively uncommon in the geological record, either due to its preservation potential or because they form more infrequently. Additionally, they are often more challenging to describe and interpret, than their finer-grained counterparts, especially in the subsurface. Sedimentological studies dealing with this type of successions are scarce, examples include the Viking and Cardium formations in the Cretaceous of Canada (Hart & Plint, 1995; MacEachern et al., 1998; MacEachern & Hobbs, 2004), the Neogene-to-Quaternary palaeostrait deposits in southern Italy (Longhitano et al., 2012), the storm dominated Miocene Sandstone of Floras Lake in SW Oregon, US (Leithold & Bourgeois, 1984) and the Late Carboniferous shallow marine conglomerates in Spitsbergen, Norway (Nemec & Steel, 1984). The coarse-grained character of the intra-Draupne Formation sandstones in the Johan Sverdrup Field promotes a rather homogeneous aspect making a detailed sedimentological interpretation and sequence stratigraphic subdivision challenging (Ottesen et al., 2022). Additional challenges lie in its limited stratigraphic thickness, (5 to 40 m), which is below seismic resolution in the area. Despite these difficulties, previous studies of the Johan Sverdrup Field developed several depositional and palaeogeographical models interpreting the deposits as wave and current reworked fan delta fronts and regolithic soils which were subsequently redeposited as different types of submarine bedforms across a shallow marine shelf (Olsen et al., 2017; Ottesen et al., 2022; Scott & Ottesen, 2018). While these works provided diagnostic criteria for interpreting the succession, there remains scope for further work that captures the facies variability and provides sequence stratigraphic correlations that form a basis for reconstructing the basin evolution and fill.

This study revisited the core material from the Johan Sverdrup Field and produced a higher-resolution sedimentological description and interpretation compared to what

Highlights

- Four laterally extensive parasequences are interpreted within the intra Draupne Formation.
- The sedimentation patterns and deposit types were strongly controlled by syn-rift topography.
- A Kimmeridgian, low-to-moderate energy lagoon existed prior to the opening of an Early Volgian tidal strait.
- Increase of the energy regime promoted the reworking of fan deltas and the formation of coarse-grained tidal barforms.
- Late Volgian-Barremian deposition was controlled by the inversion of preexisting structures.

is currently available. These were used to develop specific depositional models and a basinwide sequence stratigraphic correlation which emplaces the formation within a Late Jurassic tectonostratigraphic framework. The results of this study allow improved understanding of the coarse-grained shallow marine successions on the Utsira High and the surrounding area, which is currently under-explored. They also have implications for understanding transgressive systems on basement highs around the world.

2 | GEOLOGICAL SETTING

The Utsira High is located in the Norwegian North Sea, 150 km off the coast of Stavanger (Figure 1a). The structure is a N-S trending basement high interpreted as a Devonian-Carboniferous exhumed core complex (Phillips et al., 2019; Serck et al., 2022). It is bounded by the Mesozoic, South Viking half graben to the West (Thomas & Coward, 1996), the extensional Stord Basin to the East (Biddle & Rudolph, 1988) and the NE–SW oriented Ling Depression to the South (Olsen et al., 2017) (Figure 1b). The tectonic evolution and stratigraphic record of the Utsira High is complex and represented by the superimposition of several strata, spanning from the Palaeozoic to the Cenozoic, separated by regional unconformities. These strata were formed during different periods, including, Devonian extension and exhumation, Permo-Triassic rifting, Early-Middle Jurassic uplift and collapse of the Mid-North Sea Dome, Late Jurassic rifting and Late Cretaceous-Palaeocene inversion (Jackson & Larsen, 2008; Ottesen et al., 2022; Serck et al., 2022; Underhill & Partington, 1993). The Utsira High remained subaerially exposed from Late Triassic until the Early Cretaceous, covering an areal extension of approximately 750 km^2 during the Late Jurassic (Jørstad, 2012; Riber et al., 2015). Sedimentation was limited to narrow belts around its flanks and in intra-high grabens, such as the Triassic and Late Jurassic sedimentary infill of the Edvard Grieg and Johan Sverdrup Fields (Figure 1c) (Mahmic et al., 2018; Olsen et al., 2017; Ottesen et al., 2022). The basement of the Utsira High is mainly composed of 409–482 Ma old granites and granodiorites, and subordinate metamorphic rocks (Riber et al., 2015). Chemical and physical weathering altered and weakened the basement rocks while they were subaerially exposed, promoting the development of weathering profiles or regoliths (Riber et al., 2015). Deflation of the Mid-North Sea Dome during the Callovian, along with the onset of Late Jurassic rifting promoted rejuvenation of the highs and a regional transgression of the South Viking Graben (Jackson et al., 2010) (Figure 1c). Subsequent marine and fluvial processes were responsible for eroding and redepositing the regolith across the Johan Sverdrup Field (Riber et al., 2017; Scott & Ottesen, 2018). The main rifting phase in the Utsira High occurred during Oxfordian to Volgian times, with a reduction in extensional tectonics and subsequent inversion of pre-existing structures in the South Viking Graben during the Early Volgian to Late Albian (Jackson et al., 2010). While the Oxfordian and Kimmeridgian are regarded as periods of eustatic sea level rise, the Volgian succession, is punctuated with multiple and abrupt, tectonically driven, shoreline progradation events, as observed in the Late Jurassic short-term sea-level curve (Ottesen et al., 2022) (Figure 1c). Progradation of clastic wedges is typically correlated with periods of reduced fault activity, whereas shoreline retrogradation occurs during periods of increased or renewed rates of fault-related subsidence in pulsating rifts (Ravnås & Steel, 1998). Shallow marine and deltaic systems sourced from relatively large catchments characterized the proximal portions of the Jurassic rift system. These systems were responsible for supplying sediments to the deeper portions of the basins, where they formed gravity-flow dominated submarine complexes of channels and fans which were encased within the deep marine black shales of the Draupne Formation (Figure 1c) (Tillmans et al., 2021). Increased rates of eustatic sea level rise during the Early Cretaceous promoted a regional flooding, which drowned the previously emerged structural highs and deposited the shale-rich deposits of the Cromer Knoll Group (Figure 1c) (Copestake et al., 2003; Jackson & Larsen, 2008).

3 | BASIN CONFIGURATION AND TECTONIC STRUCTURES

The Johan Sverdrup Field is located on the east flank of the southern Utsira High. The studied region is mainly characterized by the Augvald Graben, a SE-NW oriented half-graben, which is flanked by the Haugaland High to the West and the Avaldsnes High to the East (Olsen et al., 2017) (Figure 2). The Augvald Graben is filled with sediments from Permian (or older) to Early Cretaceous age (Figure 3). Younger geological formations drape across and along the entire Johan Sverdrup Field. The pre-Cretaceous geological formations show a significant thickening towards the eastern margin of the Haugaland High, where the Main Boundary Fault (MBF), a SSE–NNW pre-Triassic structure dipping northeastwards, is located (Scott & Ottesen, 2018). Additionally, the basin is affected by multiple faults with variable orientations including the SE-NW oriented Kvalen Graben Fault (KGF) and a pair of SW–NE oriented faults, the Geitungen and Espevaer faults (GF and EF, respectively). Based on the Late Jurassic ENE-WSW stress field reported by Zanella and Coward (2003), Scott and Ottesen (2018) suggested that deformation during the Late Jurassic rifting phase was

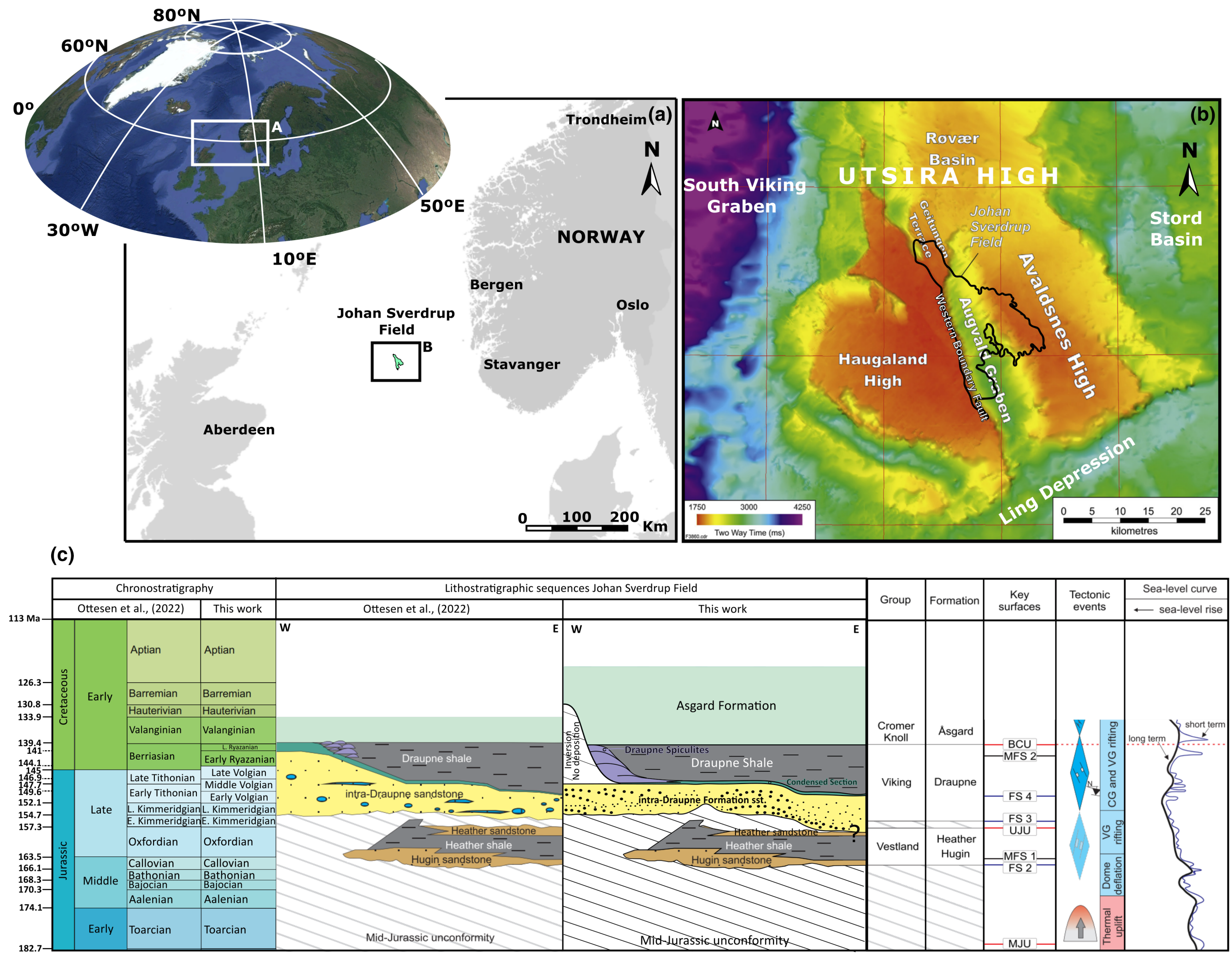

FIGURE 1 (a) Location of the study area. The extent of the Johan Sverdrup Field is depicted in light green colour and framed in the black square rectangle (globe map modified from Google Earth; local map modified from the NPD). (b) Two-way-time map of the top basement surface in the southern Utsira High (from Olsen et al., 2017). The extent of the Johan Sverdrup Field corresponds with the area within the black envelope. The Augvald Graben is bounded by the Haugaland and the Avaldsnes highs. (c) Chronostratigraphic and lithostratigraphic chart of the Johan Sverdrup Field (from Ottesen et al., 2022).

accommodated differently at each fault based on its orientation with respect to the stress field. Accordingly, the Main Boundary Fault experienced oblique slip movement, the Geitungen Fault and Espevaer Fault experienced strike-slip displacement and the Kvalen Graben Fault experienced extension (Figure 2).

4 | METHODS

A total of 22 exploration well cores were studied during 2020–21. Given the international mobility restrictions due to the global COVID-19 pandemic, a remote logging technique based on very high-resolution core images was developed. First, well-core images (provided by Lundin Energy Norway now Aker BP) were imported into Inkscape, an open-source vector drawing software. The scales were calibrated from the images, and measurements, such as grain size and bed thickness, were made using a virtual ruler, an analogous process to sedimentary logging in the core store or the field (see examples in Figure 4 of the Facies Analysis chapter). Sedimentary logs were created for each core, consisting of grain size, roundness, sorting, sedimentary structures and fossil content descriptions. Due to the homogeneity and coarse-grained character of the succession, the sedimentary logging was performed at 1:1 scale. Logging in this detail allowed the capture of all of the subtle variations in grain size, sorting, sedimentary structures and vertical stacking patterns. This in turn allowed a subdivision into facies and facies associations and a hierarchical classification of the succession in terms of bedforms and units. Age dating and palaeocurrent measurements were provided by Lundin Energy Norway and included with the sedimentary logs and regional base maps after detailed revisions and quality

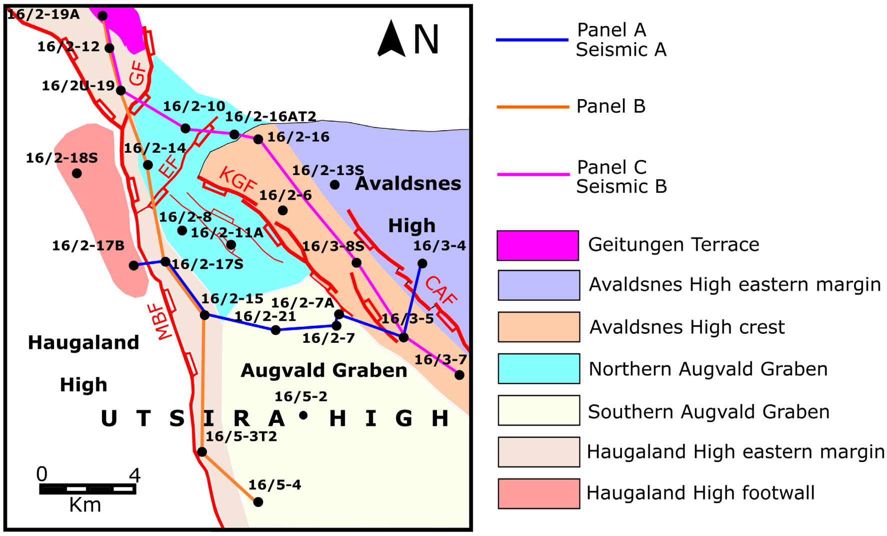

FIGURE 2 Simplified structural map of the Johan Sverdrup Field and the stratigraphic domains in which we have subdivided the description of the Late Jurassic succession in the Johan Sverdrup Field. (CAF, Central Avaldsnes Fault; EF, Espevaer Fault; GF, Geitungen Fault; KF, Kvalen graben Fault; MBF, Main Boundary Fault; NBF, Northern Boundary Fault). The location of the different well cores studied is shown. The blue-, yellow- and purple-coloured lines correspond with the seismic lines and correlation panels shown in Figures 3 and 8, respectively.

controls were performed. Fossil-based age datings were obtained from observations on palynomorphs, dinoflagellates and foraminifera among other faunal associations. The palaeocurrent data, rose plots and dip-meter readings, are obtained from formation microlog images (FMI), after the tool inclinometer data is corrected, calibrated and the structural tilt removed. Dip-meter data, for both palaeocurrent indicators and faults/fracture planes, were picked manually by an external company, Eriksfiord. The error in the measurements is 1° for the dip angle and 2°–4° on the azimuth. A well-to-well sequence stratigraphic correlation through the field, combining the lithostratigraphic, allostratigraphic and biostratigraphic data was created. 3D geophysical survey data were available and studied in-house at Lundin Energy Norway, where we interpreted multiple seismic sections in Petrel®. All the results from the stratigraphic and seismic analysis were compiled and used to create four palaeogeographical maps, which summarize the depositional history of the Draupne Formation in the Johan Sverdrup Field.

5 | RESULTS

5.1 | Seismic sections

The intra-Draupne Formation sandstones are too thin to be resolved at seismic scale, so only analysis of large-scale features is possible. The pre-Jurassic geological formations include Ordovician basement granitic rocks, Permian Zechstein carbonates, Triassic Skagerrak alluvial deposits and Upper Triassic-Lower Jurassic Eiriksson Fm. fluvial and estuarine deposits. These formations thicken towards the hanging walls of the Main Boundary Fault and Geitungen Fault (Figure 3a,b) and are significantly affected by a composite erosional surface of Middle-Late Jurassic age (Ottesen et al., 2022). This is a regional low-angle angular unconformity which mainly affects the NE and SE portions of the field, close to the Avaldsnes High (Figure 3a). At a smaller scale, the Asgard Formation thins towards the hanging wall of the Geitungen Fault (Figure 3b), where a regional anticline structure is developed. The same trend is observed close to the hanging wall of the Main Boundary Fault (Figure 3a), where another anticline structure occurs.

5.2 | Stratigraphy

The stratigraphy of the Late Jurassic-Early Cretaceous deposits has been described as subdividing the Johan Sverdrup Field in different regions (Figure 2). Thirteen different facies were described and interpreted within the Draupne Formation (which includes the intra-Draupne Formation sandstones, the Condensed Section and the Draupne Shale) and the Asgard Formation (Figures 1c and 4; Table 1). These facies are grouped in nine different facies associations (FA) (Figure 4; Table 2). Analysis of palaeocurrent data has focused on the intra-Draupne Formation sandstones (Figure 5). The facies and facies associations that characterize the intra-Draupne Formation sandstones alternate and stack vertically forming up to 4 different coarsening upward units, named 1 to 4 from the base to the top, 4 to 19 m thick each (Figure 6). Units have

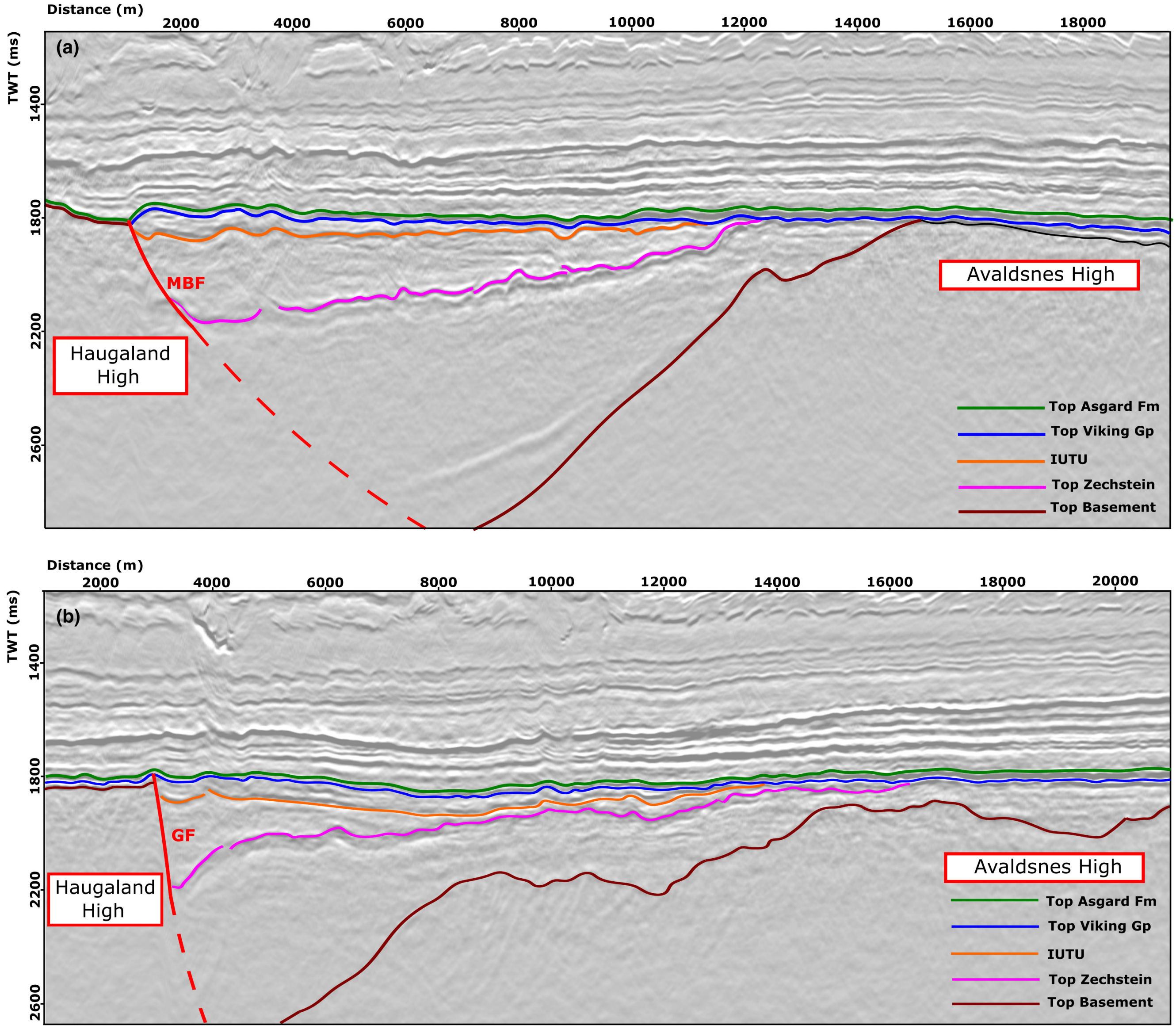

FIGURE 3 (a) Seismic line in TWT across the Augvald Graben. Note the half-graben geometry and the hanging wall anticline at the Main Boundary Fault (MBF). (b) Seismic line in TWT along the crest of the Avaldsnes High. Note the half-graben geometry and the hanging wall anticline at the Geitungen Fault (GF). Due to the extremely reduced thickness of the Jurassic interval, the whole horizon is approximated to the Top Viking Group reflector. Note the erosional character of the Viking Group reflector in the proximities of the Avaldsnes High (IUTU: Intra Upper Triassic Unconformity).

been subdivided into a basal and upper package, each dominated by massive and cross-stratified sandstones or gravels, respectively. A dark-coloured interval, termed the Condensed Section, 0.3 to 3 m. thick, separates the intra-Draupne Formation sandstones from the Draupne Shale. A series of maps and pie charts summarize the distribution

FIGURE 4 Core examples of the different facies and facies associations. (a) Rippled and laminated muddy sandstones interbedded with gravel beds, FA-1, and (b) cross-stratified sandstones (FA-2). Note the intense bioturbation by Macaronichnus segregatis. (c) Massive sandstones. (d) Erosional, cross-stratified, fining upwards bedsets of FA-3. Note the presence of Skolithos burrows displaying escape structures. (e–h, j) Coarsening upwards bedsets of bidirectional cross-stratified sandstones and gravels, FA-5. (i) Bidirectional cross-stratified gravels embedded within massive sandstones. (k) Massive coarsening upwards sandstones and gravels, FA-4. (l) Bedsets of alternating structureless gravel beds and massive sandstones, FA-6. (m, n) Dark-coloured, nodule and belemnite-rich deposits of the Condensed Section, FA-7. (o) Massive and thinly laminated black shales of the Draupne Shale, facies Shb. (p, q) Interbedded spiculitic sandstones and shales, FA-9. (r) Interbedded spiculitic sandstones and gravels, FA-8. (s, v, w) Base of the intra-Draupne Formation sandstones affected by Thalassinoides and other unidentified traces. (t, u) Red and green shales of the Asgard Formation, facies Shg.

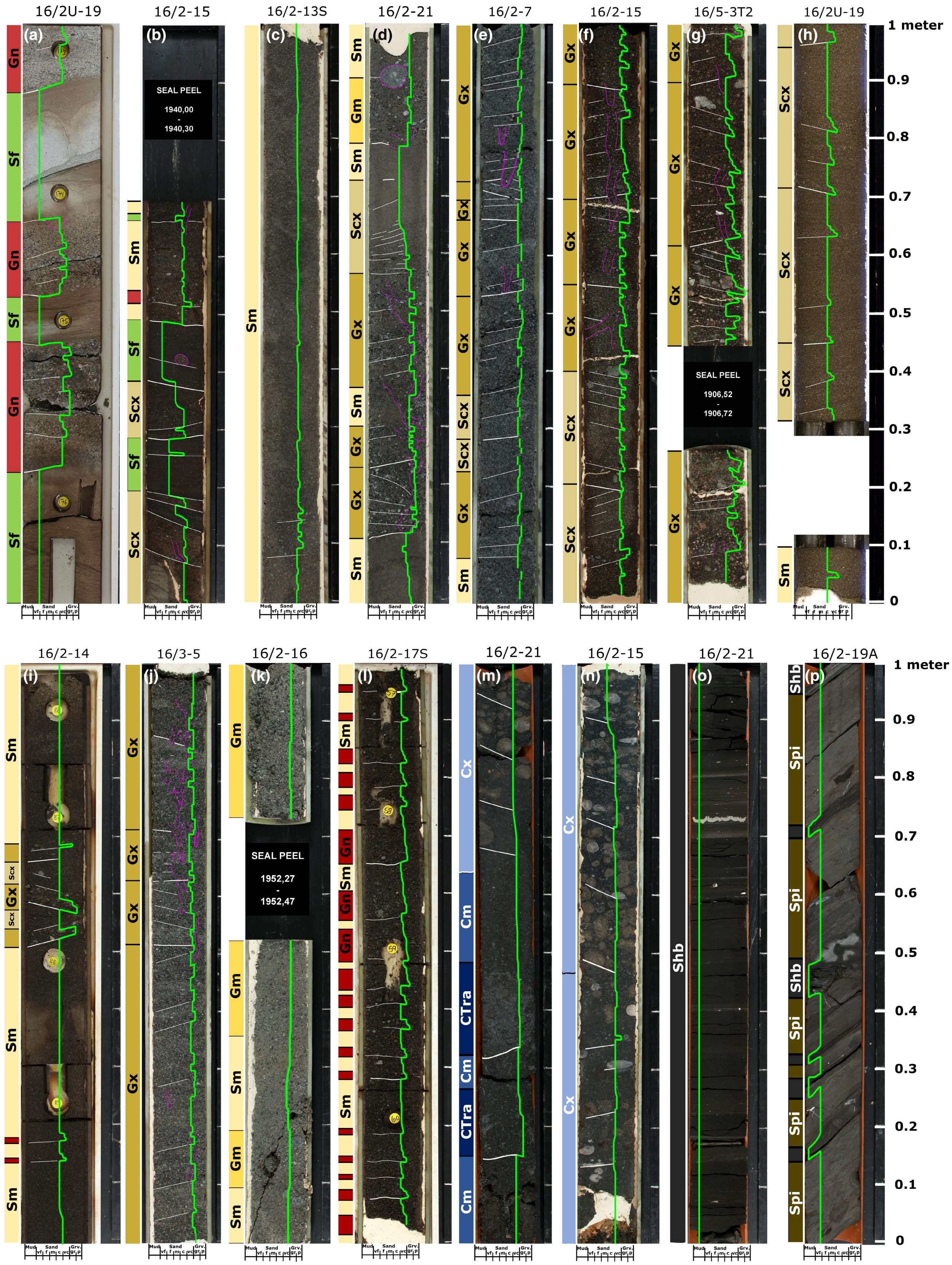
16/2U-19
16/2-15
16/2-13S
16/2-21
16/2-7
16/2-15
16/5-3T2
16/2U-19
(a)
(b)
(c)
(d)
(e)
(f)
(g)
(h)
Gn
Sf
Gn
Sf
Gn
Sf
SEAL PEEL
1940,00
-
1940,30
Sm
Sf
Scx
Sf
Scx
Sm
Sm
Gm
Sm
Scx
Gx
Sm
Gx
Gx
Sm
Gx
Gx
Gx
Gx
Gx
Scx
Scx
Gx
Sm
Gx
Gx
Gx
Gx
Gx
Scx
Scx
Gx
Gx
Gx
SEAL PEEL
1906,52
-
1906,72
Gx
Scx
Scx
Scx
Sm
1 meter
0.9
0.8
0.7
0.6
0.5
0.4
0.3
0.2
0.1
0
16/2-14
16/3-5
16/2-16
16/2-17S
16/2-21
16/2-15
16/2-21
16/2-19A
(i)
(j)
(k)
(l)
(m)
(n)
(o)
(p)
Sm
Scx
Gx
Scx
Sm
Sm
Gx
Gx
Gx
Gx
Gm
SEAL PEEL
1952,27
-
1952,47
Gm
Sm
Gm
Sm
Sm
Gn
Sm
Gn
Gn
Sm
Cx
Cm
CTra
Cm
CTra
Cm
Cx
Cx
Shb
Shb
Spi
Spi
Shb
Spi
Spi
Spi
1 meter
0.9
0.8
0.7
0.6
0.5
0.4
0.3
0.2
0.1
0

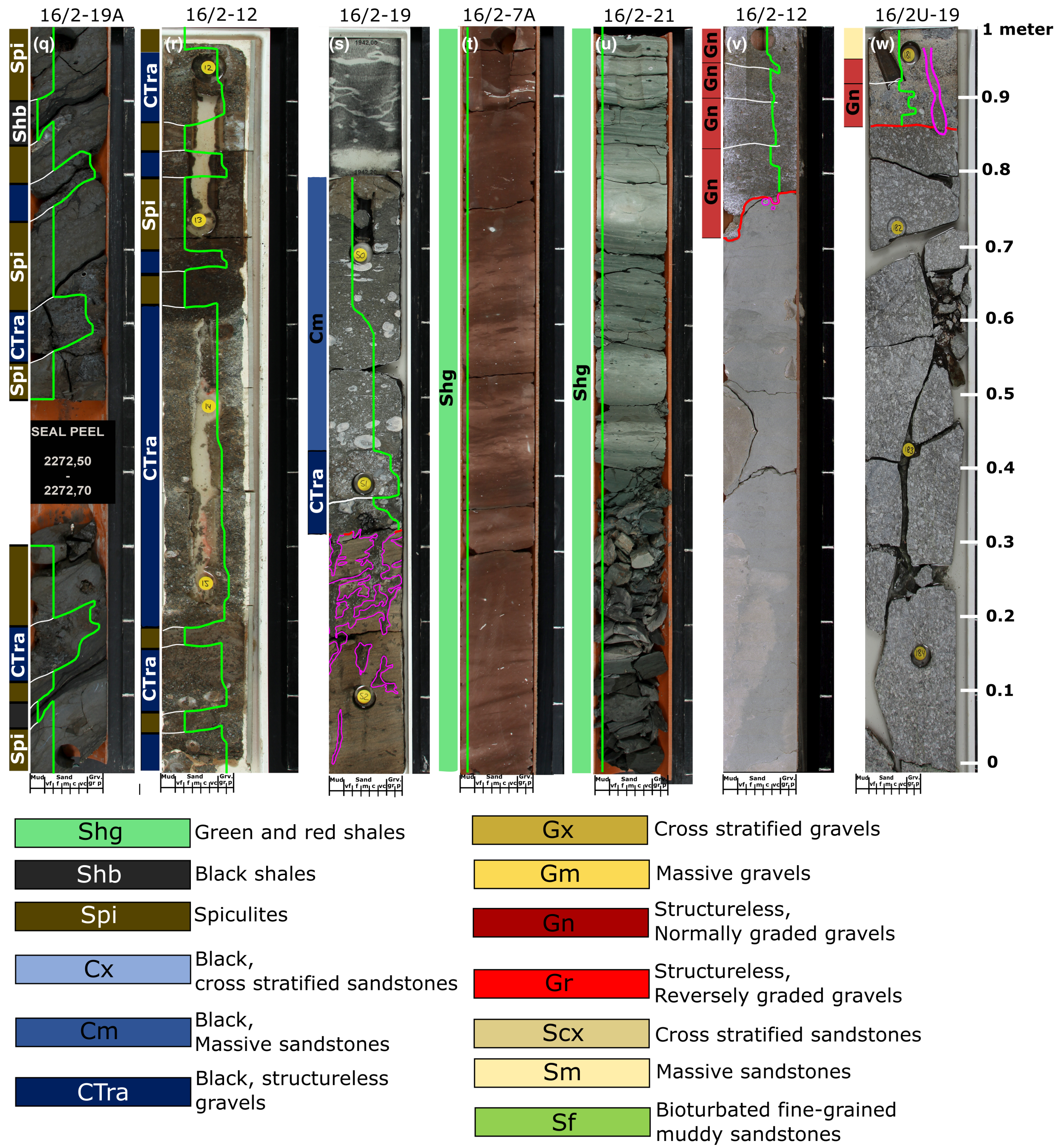

FIGURE 4 (Continued)

of the main facies types through the different units and geological formations (Figure 7).

5.2.1 | Palaeocurrent analysis

Palaeocurrent data from dip-meter readings within the intra-Draupne Formation sandstones reveal highly bidirectional palaeoflows (Figure 5). Dip of the palaeocurrent measurements is usually comprised between 5° and 15°, up to 25°, locally (Figure 5). Palaeocurrent directions in the Augvald Graben and specially, in the Haugaland High eastern margin, are consistent and mainly orientated NNE–SSW, slightly oblique to the axis of the graben and to the strike of the Main Boundary Fault (Figure 5). Dip-meter data show a slight dominance of northwards or southwards-directed palaeocurrents towards the respective tips of the Main Boundary Fault, wells 16/2-12, 16/2-15

TABLE 1 Facies catalogue.

Facies	Grain texture and bioturbation	Sedimentary structures and bed thickness	Interpretation
Shg	Well-to-very well-sorted, green and red coloured shales of the Asgard Formation. Bioturbated by *Planolites*, *Thalassinoides* and other cryptic burrowers	Massive or showing millimetre scale thin laminations of lighter-coloured shale or slightly siltier and sand-prone laminates	Pelagic shales reflecting background sedimentation. These are deposited after the drowning of the nearby clastic source areas in a deep marine shelf
Shb	Well-to-very well-sorted black-coloured shales of the Draupne Formation. Bioturbated by *Planolites, Thalassinoides* and other cryptic burrowers	Massive or showing millimetre scale thin laminations of lighter-coloured shale or slightly siltier and sand-prone laminates. Beds are 1 to 15 cm thick when they are interbedded with the spiculitic facies	Pelagic shales reflecting background sedimentation. These are deposited after the drowning of the nearby clastic source areas in a deep marine shelf
Spi	Poorly-to-very well-sorted spiculitic fine-grained sandstones with variable amounts of floating granules and belemnites. Attributed to the Draupne Formation. Might be intensely bioturbated by *Planolites* and *Thalassinoides*, completely destroying the original fabric	Whenever the original fabric is preserved, spiculitic beds show millimetre scale sub-horizontal laminations, ripples or a massive aspect. Spiculitic beds are 3 to 15 cm thick. Bed boundaries might be diffuse due to amalgamation. Amalgamated packages might reach up to 1 m in thickness	Current reworked siliceous sponge reefs redeposited during a period of low clastic input in a relatively deep marine shelf
Cx	Moderate-to-poorly sorted, dark-coloured, fine-to-coarse-grained sandstones very rich in floating gravels, septarian nodules and belemnites. This facies is typically found at the top of the condensed section, directly underneath the Draupne Formation	Bidirectional cross-stratification. Beds are 5 to 20 cm thick	Ebb and flood current generated submarine dunes formed during a period of low clastic input and sediment starvation in a relatively low-to-moderate energy deep marine shelf
Cm	Moderate-to-poorly sorted, dark-coloured, fine-to-coarse-grained sandstones rich in septarian nodules and belemnites	Massive	Condensation package reflecting low sedimentation rates and sediment starvation during the transition from shallow marine conditions to a progressively deeper marine shelf
CTra	Moderate-to-poorly sorted, dark-coloured, granules and pebbles with variable amounts of coarse-to-very coarse sandstone, belemnites and septarian nodules. This facies is typically found within or at the base of the condensed section	Massive or normally graded. If it is found at the base of the condensed section it typically forms a 10 to 20 cm thick amalgamated deposit	Transgressive lag and gravity flow deposits formed as the result of a regional relative sea level rise which drowned the majority of the clastic source areas
Gx	Moderately-to-well-sorted granules and pebbles, locally poorly sorted. Interlaminated well-to-very well-sorted coarse-to-very coarse-grained sandstones appear subordinately. Burrowed by *Skolithos* showing escape traces	Bidirectional cross-stratification. Beds are 3 to 25 cm thick, displaying coarsening and finning upward patterns. Beds are internally laminated, showing mm to 2 cm thick laminates of alternating granules, pebbles and sandstones	Ebb and flood gravelly dune deposits generated under strong axial or alongshore currents in a shallow marine shelf

(Continues)

TABLE 1 (Continued)

Facies	Grain texture and bioturbation	Sedimentary structures and bed thickness	Interpretation
Gm	Moderate-to-poorly sorted granules and pebbles. Bioturbated by *Skolithos*, sometimes displaying escape traces	Massive. Beds are 2 to 15 cm thick whenever they are interbedded with other facies. Otherwise, this facies might be in transitional contact with the underlying or overlying facies, showing no clear boundary between beds or facies type	Gravity flow deposit, wave generated/ wave reworked submarine barform foreset or massive due to bioturbation
Gn	Moderate-to-poorly sorted granules and pebbles. Bioturbated by *Skolithos*, sometimes displaying escape traces	Normal grading. Beds are 1 to 20 cm thick	Gravity flow deposit
Gr	Moderate-to-poorly sorted granules and pebbles. Bioturbated by *Skolithos*, sometimes displaying escape traces	Reverse grading. Beds are 2 to 15 cm thick	Gravity flow deposit
Scx	Moderate-to-very well-sorted, medium-to-very coarse-grained sandstone. Moderately-to-well-sorted granules may appear locally within beds. Burrowed by *Skolithos* showing escape traces	Bidirectional cross-stratification. Beds are 5 to 25 cm thick, displaying coarsening and finning upward patterns. Beds are internally laminated, showing mm to 2 cm alternating laminates of sandstone and granules, locally	Ebb and flood sandy dune deposits generated under strong axial or alongshore currents in a shallow marine shelf
Sm	Moderate-to-very well-sorted, medium-to-very coarse-grained sandstones. Bioturbated by *Skolithos*	Massive. Beds are 2 to 15 cm thick whenever they are associated with other facies; however, it is more common to find them amalgamated forming meter thick massive packages	Background sedimentation, interdune/interbar deposits formed in areas of weaker current activity, wave generated/ wave reworked submarine barform bottomset or massive due to bioturbation
Sf	Well-to-very well-sorted fine-grained sandstones. Intensely bioturbated by *Macaronichnus segregatis* and, subordinately, *Thalassinoides*	Sedimentary structures include symmetric and slightly asymmetric ripples with mud drapes and horizontal, mm to 1 cm thick, interlaminated fine-grained sandstones and muds. Massive sometimes due to intensive bioturbation. Beds are 1 to 60 cm thick	Tidal influenced rippled upper shoreface characteristic of a low-to-moderate energy shallow marine environment

TABLE 2 Facies association catalogue.

Facies associations	Description	Interpretation	Graphic log
FA-9	Fine-grained spiculitic sandstones (facies Spi) interbedded with massive black shales (facies Shb). Non-apparent vertical trends. Bioturbated by *Thalassinoides, Planolites* and cryptic burrowers	Reworked siliceous sponges redeposited close to inactive feeder systems or far offshore in a starved shelf	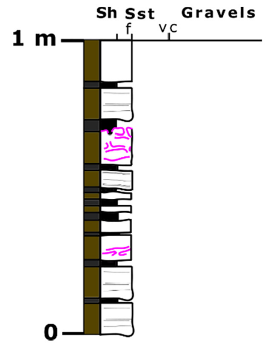
FA-8	Fine-grained spiculitic sandstones (facies Spi) interbedded with massive or normally graded, moderate-to-poorly sorted granules and pebbles very rich in belemnites and septarian nodules (Facies CTra). Non-apparent vertical trends. Bioturbated by *Thalassinoides, Planolites* and cryptic burrowers	Reworked siliceous sponges redeposited close to an active fan delta system in a starved shelf	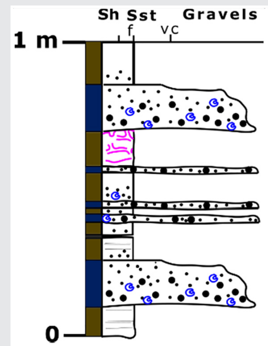
FA-7	Dark-coloured, poorly sorted nodule and belemnite-rich gravels (Facies CTra) passing upwards to dark-coloured, moderately-to-poorly sorted, fine-to-very coarse-grained massive sandstones (facies Cm), and locally, cross-stratified nodule rich sandstones in the uppermost part of the section (facies Cx)	Condensed section indicating low sedimentation rates. The section is generated during the drowning of the clastic source areas following a regional relative sea level rise. Current circulation in the basin might still be active as suggested by the presence of cross-stratified deposits	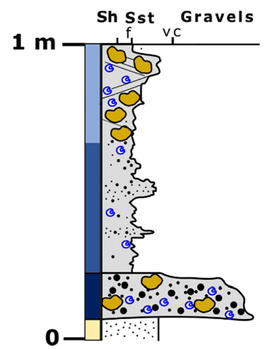

(Continues)

TABLE 2 (Continued)

Facies associations	Description	Interpretation	Graphic log
FA-6	Coarsening and finning upwards bedsets, 0.5–2.2 m thick, of alternating massive, normally or reversely graded, moderately-to-poorly sorted granules and pebbles beds (facies Gm, Gn and Gr) and moderately-to-well-sorted massive coarse-to-very coarse-grained sandstones (Sm). Bioturbated by *skolithos* showing escape traces	Gravity flow dominated progradational and retrogradational submarine fan delta lobes deposited in a low, moderate or high energy environment	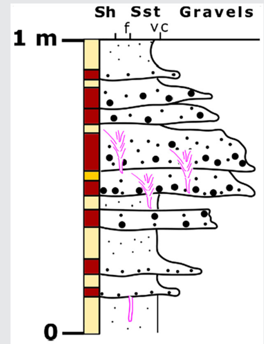
FA-5	Bidirectional cross-stratified coarsening and finning upwards bedsets, 0.5–2.2 m thick, consisting of a basal well-to-very well-sorted, coarse-to-very coarse-grained sandstone member (facies Scx) passing vertically to a moderately-to-well-sorted granule and pebble dominated upper member (facies Gx). Bioturbated by *skolithos* showing escape traces	Bidirectional cross-stratified barforms generated as a consequence of fan delta front and regoliths reworking under strong ebb and flood axial or alongshore currents	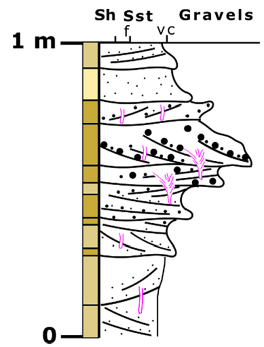
FA-4	Massive, coarsening and finning upwards bedsets, 0.5–1.5 m thick, characterized by a basal member consisting of moderate-to-very well-sorted, coarse-to-very coarse-grained sandstones (facies Sm) passing transitionally to an upper member consisting of massive, moderately-to-well-sorted granules and pebbles (facies Gm). Bioturbated by *skolithos* showing escape traces	Wave generated nearshore and swash bars or wave reworked current generated barforms	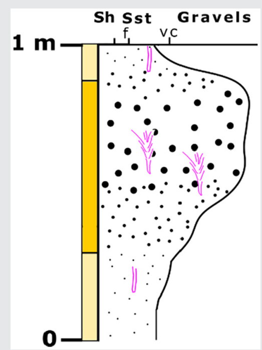

TABLE 2 (Continued)

Facies associations	Description	Interpretation	Graphic log
FA-3	Highly erosional finning upwards bedsets, 0.2 to 0.7 m thick, consisting of a basal member dominated by bidirectional cross-stratified deposits of facies Gx and, subordinately, facies Gm and Gn. The upper member is dominated by massive or cross-stratified lower coarse-to-very coarse-grained sandstone beds of facies Sm and Scx. Multiple vertical burrows showing escape traces are found at the base of each bedset, sometimes destroying the original fabric and promoting a rather structureless fabric	Channel fill. Bedforms migrate within an active channel which is progressively abandoned. Its offshore position and the proximity to the Avaldsnes spit suggest these are tidal channels	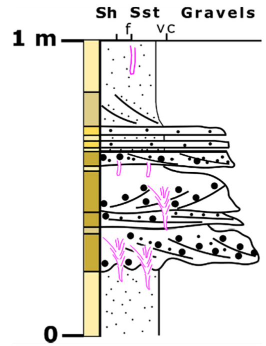
FA-2	Bidirectional cross-stratified very well-sorted lower coarse-to-very coarse-grained sandstones (facies Scx) interbedded with bioturbated fine-grained sandstones (facies Sf) forming up to 0.5 m thick cross-stratified bedsets. Bioturbated by *Macaronichnus* and *Thalassinoides*	Tidal influenced upper shoreface barforms generated under low-moderate energy currents	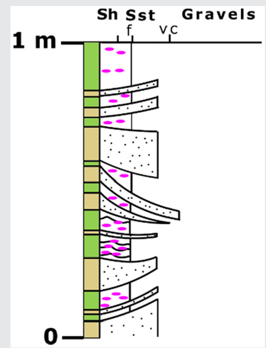
FA-1	Interbedded bioturbated fine-grained sandstones (facies Sf) and massive or normally graded moderate-to-poorly sorted granules and pebbles (facies Gm, Gn and Gr). Contact between both facies tends to be abrupt. Gravel bed's basal boundary is sharp or slightly erosional. Bioturbated by *Macaronichnus* and *Thalassinoides*	Gravity flow submarine fan delta lobes deposited in a shallow marine, low-to-moderate energy fine-grained upper shoreface	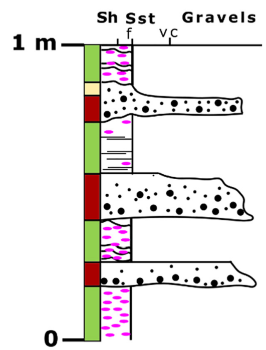

and 16/5-3T2, whereas a zone of co-dominant readings or indistinct dominant phases is observed around wells 16/2-8 and 16/2-14. Additionally, wells located close to the fault tips tend to show gentler dipping dip-meter data, 2° to 7°, compared with wells 16/2-8 and 16/2-14, which show steeper readings, most of them dipping between 15° and 25° (Figure 5). Further East, in the Avaldsnes High, there is predominance of NW-SE bidirectional palaeocurrents, which parallel the crest of the Avaldsnes High and show no dominant phase (Figure 5). This trend is locally interrupted towards the northeast and southeast, close to wells 16/2-16AT2 and 16/3-5, respectively, where palaeocurrents are almost perpendicular to the trace of the Avaldsnes High and show a marked NE–SW bidirectionality or a more unimodal trend towards either one of these directions, as in wells 16/2-10, 16/2-7 and well 16/3-4 (Figure 5). Subordinate NE-directed palaeocurrents overprint the general trends described in both the Haugaland eastern margin and the crest of the Avaldsnes High. Although palaeocurrents are unevenly sampled within and between wells, it is still possible to observe clusters of cross-beds, 0.5 to 2.5 m thick, with similar values. These clusters are common in the majority of the wells and alternate vertically showing bidirectionality at bedset scale (Figure 5, wells 16/2-8, 16/2-21, 16/3-8S and 16/3-5). Although bidirectionality at unit scale is well recorded in log 16/2-14, suggesting a northwards dominated component in units 2 and 4, and a southwards dominance in unit 3, the sampling distribution of the palaeocurrent data did not allow a regional analysis of any clear variation or shift in the palaeocurrent trends at this scale.

5.2.2 | Facies analysis

No deposits of the Draupne Formation were found on top of the Haugaland High footwall. Unit 1 of the intra-Draupne Formation sandstones is the most variable in facies and extent. It is absent in the southernmost part of the Augvald Graben and at some local wells in the crest of the Avaldsnes High (Figures 6 and 7a). Fine-grained muddy sandstones intensively bioturbated by *Macaronichnus Segregatis* (facies Sf) characterize the lower package of Unit 1 and occupy a narrow belt parallel to the Haugaland High (Figure 7a). There, they are interbedded with either normally or reversely graded gravel beds (FA-1, Figure 4a)

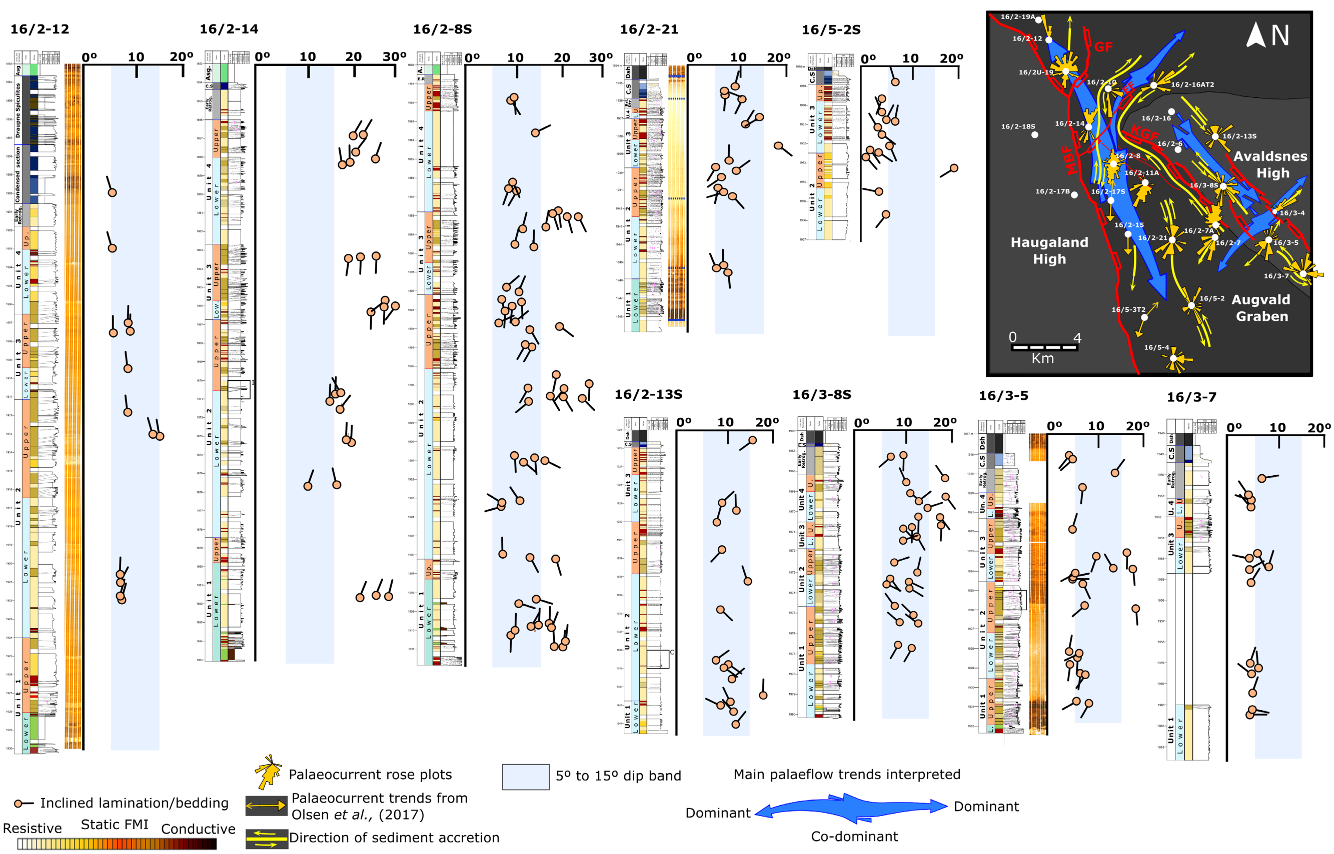

FIGURE 5 Dip-meter data and palaeocurrent rose diagrams intercepted with the stratigraphic logs of the intra-Draupne Formation sandstones. Palaeocurrent data is highly bidirectional, with dips comprised between 5° and 15°, locally up to 25°. Palaeoflow directions are interpreted based on the dominant palaeocurrent trends and our interpretation of the facies.

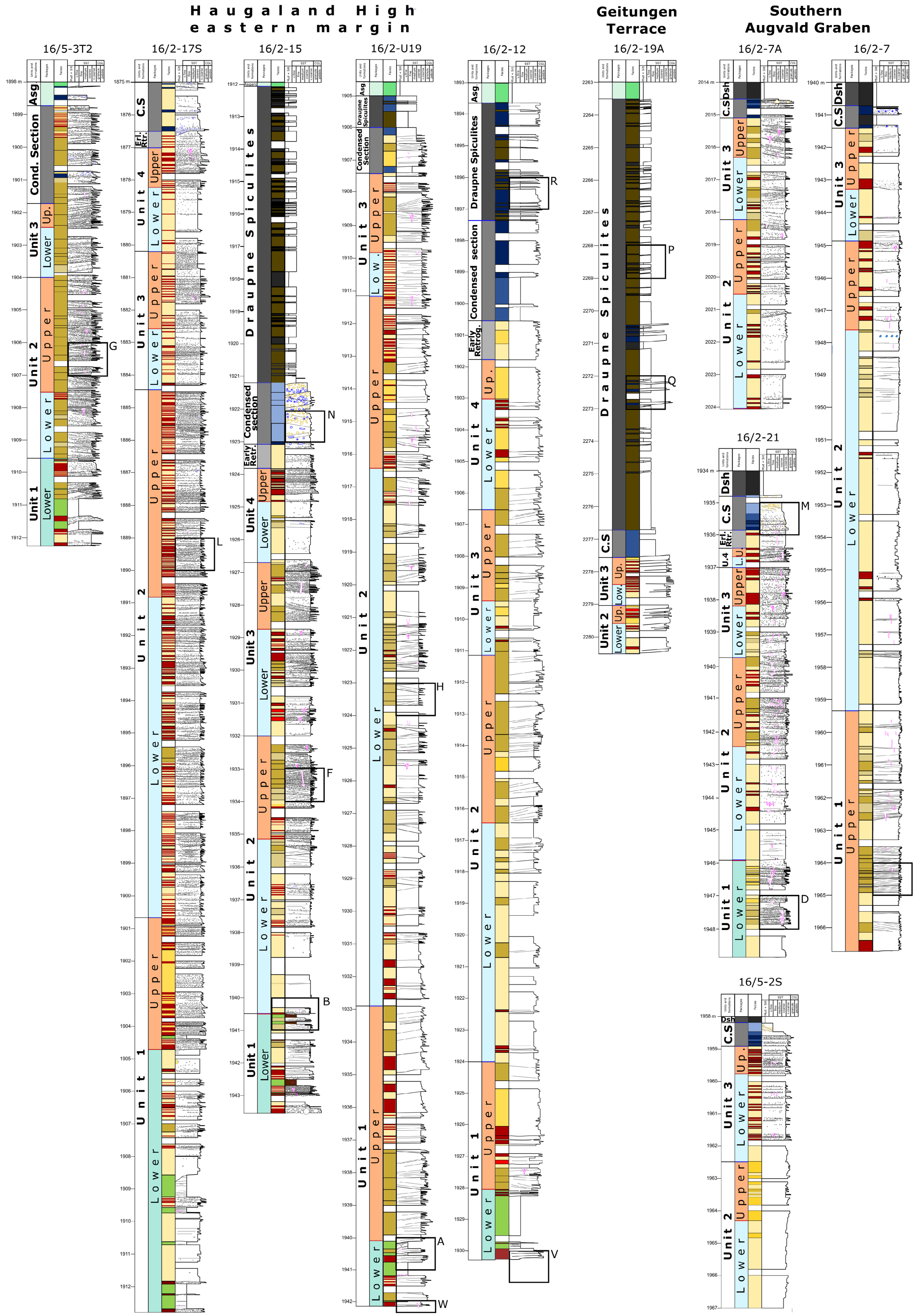

FIGURE 6 Sedimentary logs resulting from the 1:1 well-core descriptions of the intra-Draupne Formation sandstones. The stratigraphic succession has been described and subdivided in terms of units, packages and facies. Colour code for facies is located in Table 1. Colour code for the Units is located in Figure 8. Black square boxes correspond to the position of the different images shown in Figure 4.

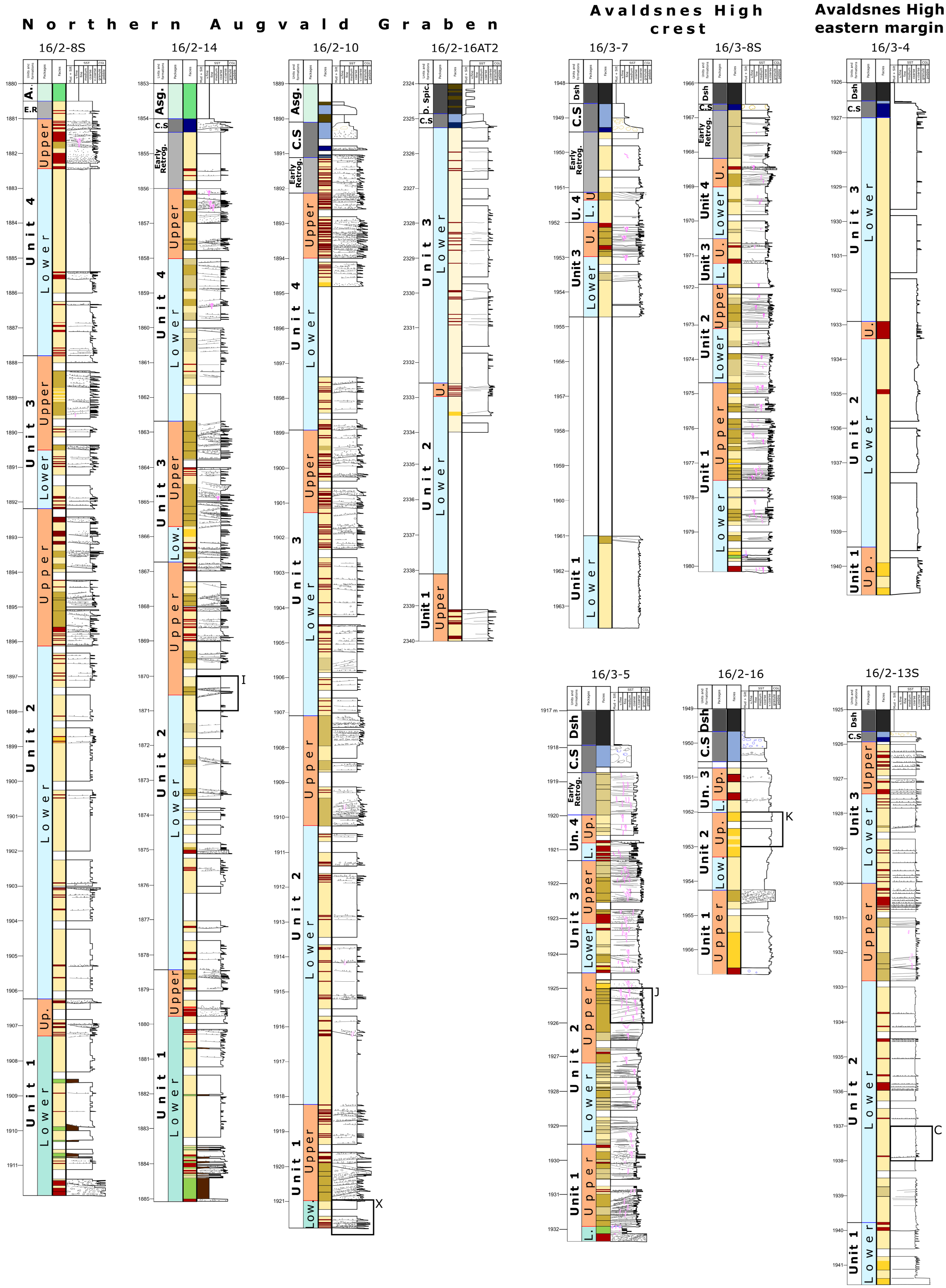

FIGURE 6 (Continued)

or massive, locally cross-stratified, very coarse-to coarse-grained sandstones (FA-2, Figure 4b), interpreted as gravity flow deposits and small tidal bedforms formed in a low-to-moderate energy upper shoreface. Facies Sf disappears laterally towards the inner portions of the Augvald Graben and the eastern margin of the Avaldsnes High, into a region with little sediment variability, dominated by massive, very coarse-to coarse-grained sandstone intervals (Figures 4c and 7a). Exceptions occur in wells 16/2–21 and 16/2–7 of the southern Augvald Graben, characterized by bidirectional cross-stratified gravel and very coarse-to coarse-grained sandstone deposits which occur as erosional-based, upward fining bedsets in well 16/2-21 (FA-3, Figure 4d) or cross-stratified coarsening upwards bedsets in well 16/2-7 (FA-5, Figure 4e), interpreted as tidal inlets and inter-channel tidal bar deposits, respectively (Figures 5 and 6). The lower packages of the overlying units, units 2–4, are characterized by massive and bidirectional cross-stratified very coarse-to coarse-grained sandstones (Figures 4c,h,i and 7b), whereas the upper packages are dominated by granules and pebbles (Figure 4e–g,j,k). These units lack the bioturbated fine-grained muddy sandstones and are mainly bioturbated by *Skolithos*, usually showing escape traces, indicating rapidly shifting seafloor sedimentation. The gravel content and grain size is higher at the eastern margin of the Haugaland High and at the crest of the Avaldsnes High, from where it tends to reduce laterally, towards the Augvald Graben and the eastern margin of the Avaldsnes High (Figures 6 and 7b). Coarsening and fining upwards bedsets composed of interbedded massive sandstones and structureless, normally graded gravel beds, dominate the

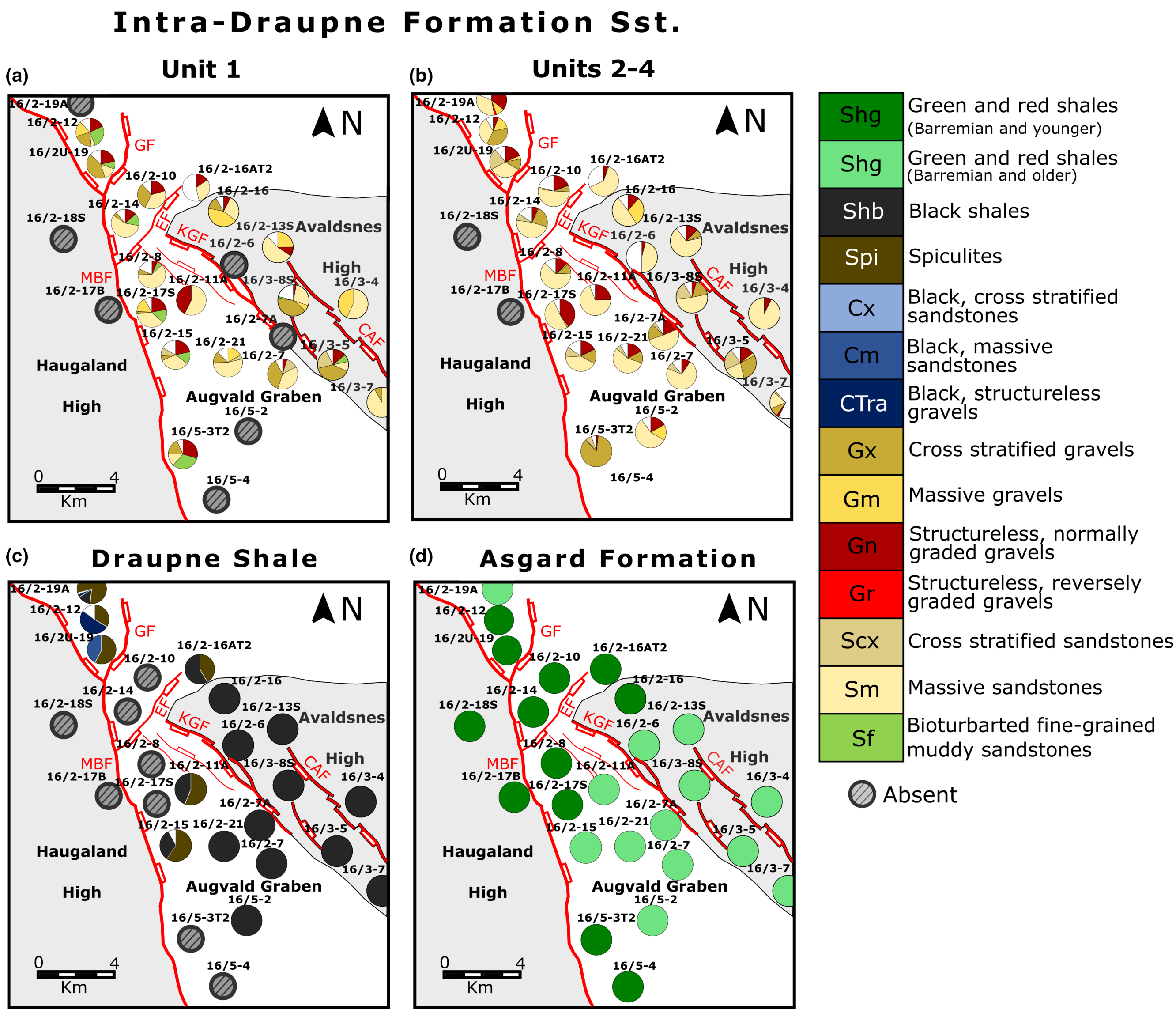

FIGURE 7 Facies distribution maps. Maps and pie charts show the distribution of the different facies which characterize the multiple parasequences at each well and that have implications for later palaeogeographical reconstructions.

inner portions of the Augvald Graben and well 16/2-17S of the Haugaland High eastern margin, and are interpreted as progradational and retrogradational fan delta lobes (FA-6, Figure 4l). Bidirectional NNE–SSW and NW-SE cross-stratification is specially well developed in wells paralleling the Haugaland High and those at the crest of the Avaldsnes High, respectively (Figures 5–7b). These regions are characterized by coarsening and fining upwards bedsets, 0.5 to 2 m thick, of alternating bidirectional cross-stratified sandstones and gravels, interpreted as reworked regoliths and fan delta fronts which were mainly deposited as tidal bars, simple/compound dunes and gravel spit deposits (FA-5, Figures 4f–i,j and 6). Similar coarsening upwards bedsets in well 16/2-16 of the Avaldsnes High, composed of structureless and gradational deposits, are interpreted as wave-generated bars or highly bioturbated tidal bedforms (FA-4, Figure 4k). Deposits of Unit 4 are dominated by the same facies associations, FA-4, FA-5 and FA-6; however, they are relatively finer-grained than those in underlying units 2 and 3. Additionally, they are only recorded in some wells, immediately attached to the main faults, specially, the Geitungen and Espevaer Faults (Figure 6) (see Sequence Stratigraphy chapter). Where present, deposits in unit 4 grade transitionally into a well-developed fining upwards interval, 0.5 to 1.5 m thick, composed of massive sandstones, locally dark in colour, which is described and interpreted as an early retrogradational interval (Figure 6). The Condensed Section is present in all wells and was deposited on top of the intra-Draupne Formation sandstones and immediately below the Draupne Shale. It is characterized by poorly sorted and dark-coloured, nodule and belemnite-rich deposits (Figure 4m,n), stacked forming a threefold division (FA-7) consisting of (i) a basal conglomeratic layer (Facies CTra), (ii) a middle interval of massive sandstones (Facies Cm) and (iii) an upper interval of cross-stratified coarse-to-fine-grained sandstones (Facies Cx) where nodules and belemnites are concentrated in higher amounts, all indicating conditions of sediment starvation (Figure 6). Exceptions occur in well 16/2-19A of the Geitungen Terrace, where the Condensed Section deposits change laterally to fine-grained spiculitic sandstones (Facies Spi). A similar behaviour is observed in the overlying Draupne Shale, which is mainly characterized by massive and dark-coloured black shales (Facies Shb, Figures 4o and 7c). Exceptions occur around the anticline structures as identified in Figure 3, where fine-grained spiculitic sandstones of the Draupne Shale appear associated with gravels (FA-8, Figure 4r) and black shales (FA-9, Figure 4p,q), and interpreted as sponge fragments redeposited in the proximal portions of a sediment-starved shelf (Figures 6 and 7c). These facies dominate the stratigraphic succession of the Geitungen Terrace, where the intra-Draupne Formation sandstones are mostly or completely absent, as in well 16/2-19. Instead, a thin interval, 0.5 m thick, corresponding to the Condensed Section rests unconformably on top of the Statfjord group, which is highly bioturbated by *Thalassinoides*, penetrating up to 30 cm down into the underlying strata (Figure 4s).

The Early Cretaceous Asgard Formation, characterized by green and red shale deposits (Facies Ash, Figure 4t,u), is deposited on top of the Draupne Shale, or if absent, the intra-Draupne Formation sandstones (Figure 7d).

5.3 | Sequence stratigraphy

5.3.1 | Significance of depositional units and their bounding surfaces

The intra-Draupne Formation sandstones are relatively thin, although they are correlatable throughout most of the Johan Sverdrup Field (Figure 8a–c). The intra-Draupne Formation sandstones thicken towards the hanging wall of the Main Boundary Fault and Geitungen Fault, attaining a maximum thickness of 40 m, and thin towards the crest of the Avaldsnes High, displaying a clear wedge geometry in cross-section (Figure 8a). Similarly, they display a synform geometry along the trace of the Main Boundary Fault, wedging out progressively towards the South and the North, as they approach the fault tips (Figure 8b), all together indicating syn-depositional growth due to fault-related subsidence. The base of the intra-Draupne Formation sandstones is a low-angle erosional unconformity as seen in the seismic data since it appears to truncate the underlying reflectors and from the variety of sub-cropping geological formations (Figure 3). This unconformity is interpreted as a surface of marine transgression based on the presence of Late Jurassic intra-Draupne Formation marine deposits overlying much older fluvial and estuarine Lower Jurassic deposits, alluvial Triassic deposits, Permian carbonate rocks and Ordovician granitoids (Figure 3). The surface is associated with extensive *Thalassinoides* and other firm ground traces, which suggest the deposits were at least semi-lithified prior to erosion and burrowing (Figure 4s,v,w). The stratigraphy of the intra-Draupne Formation sandstones has been subdivided into 4 main units, which are vertically stacked and bounded by regional surfaces, separating gravel-rich marine sediments below from finer-grained sediments above in all the units. These surfaces are recognized as sharp and subhorizontal discontinuities throughout most of the basin, despite the surface between units 1 and 2 tends to be slightly transitional in the immediate hanging wall of the Main Boundary Fault (Figure 6, wells 16/2-17S, 16/2-12 and 16/2U-19). The intra-Draupne Formation sandstones are Oxfordian to Middle Volgian in age. Unit 1 is mainly

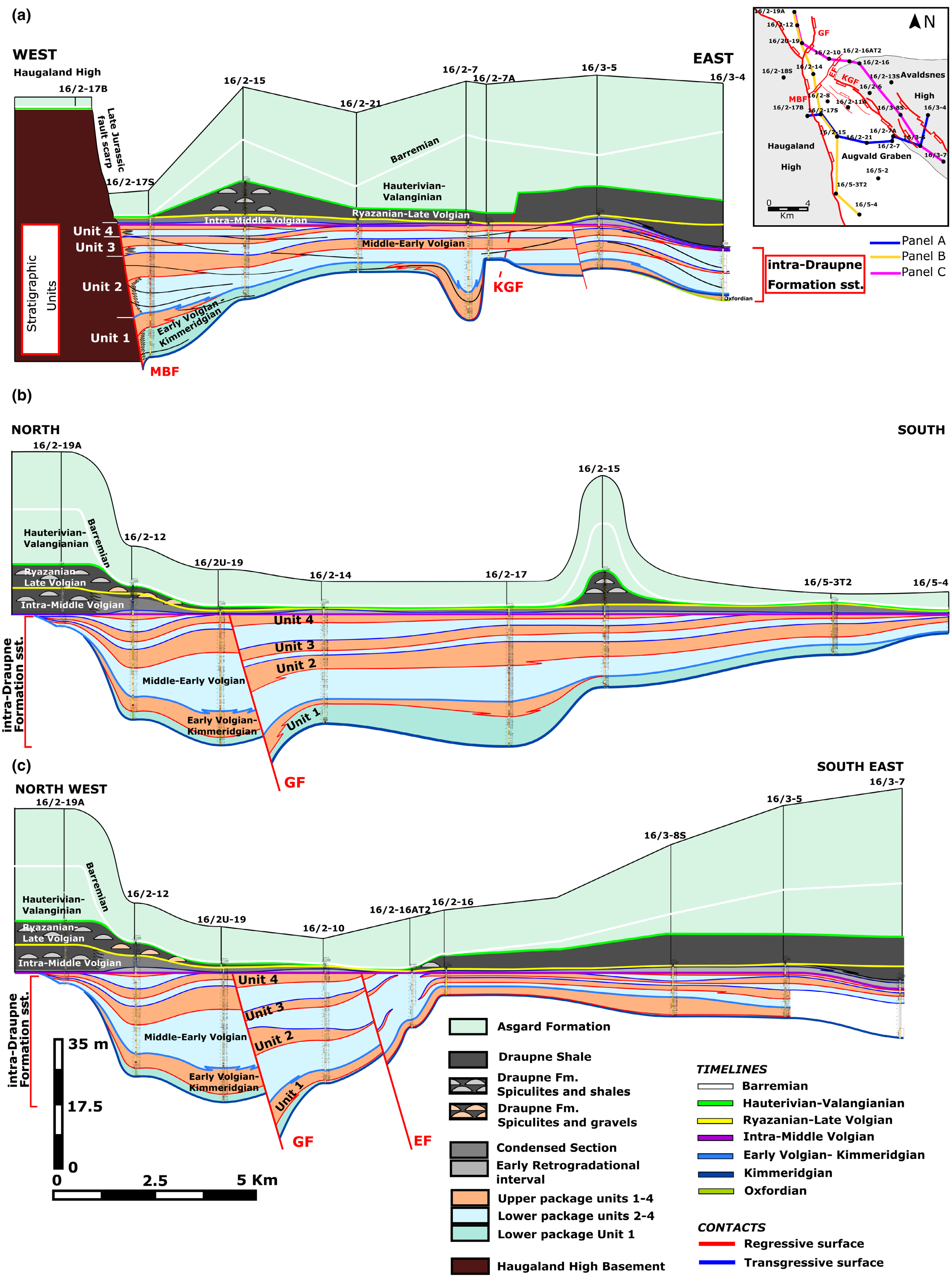

FIGURE 8 (a) Correlation panel across the Augvald Graben. (b) Correlation panel along the hanging wall of the Main Boundary Fault. (c) Correlation panel along the crest of the Avaldsnes High. EF, Espevaer Fault; GF, Geitungen Fault; KGF, Kvalen Graben Fault; MBF, Main Boundary Fault.

dated as Kimmeridgian-Early Volgian, while Units 2, 3 and 4 date as Early to Middle Volgian. Biostratigraphic dating suggests that these units are younger basinwards, towards the Augvald Graben and the Avaldsnes High eastern margin, especially units 2, 3 and 4. These become younger away from the Haugaland and Avaldsnes highs, characterized by Early Volgian dates, towards the southern Augvald Graben, where they are dated as Middle Volgian, mainly (Figure 8a). The grain size distribution also shows a fining from the Haugaland and Avaldsnes Highs towards the Augvald Graben or the eastern margin of the Avaldsnes High. These observations suggest that the boundaries between units are regional flooding surfaces and that units 1 to 4 are actually four individual progradational parasequences (parasequences 1–4) (sensu Van Wagoner et al., 1988). The base of the early retrogradational interval which fines upwards and grades from the underlying unit 4, is interpreted as a transitional surface, formed locally, prior to the deposition of the overlaying Condensed Section, mainly during the Middle Volgian. In the absence of the Early Retrogradational interval, the boundary between Unit 3 or 4 and the dark-coloured Condensed Section is an abrupt and very distinguishable discontinuity, interpreted as a regional transgressive surface. The surface between the Condensed Section and the Draupne Shale is a sharp and abrupt discontinuity, formed as the transgression advanced and onlapped onto the Haugaland High, during the Late Volgian-Ryazanian. Finally, the contact between the Late Jurassic Draupne Formation and the Early Cretaceous green-red shaly deposits of the Asgard Formation is a sharp, subhorizontal discontinuity interpreted as the Base Cretaceous Unconformity (BCU), which dates as Valanginian-Hauterivian throughout most of the basin, up to Barremian, locally, on top and along the eastern margin of the Haugaland High.

5.3.2 | Oxfordian deposits in the Avaldsnes High eastern margin

Oxfordian dates are limited to the crest of the Avaldsnes High and its eastern margin (i.e., wells 16/2-13S, 16/3-7, 16/3-8S and 16/2-16), where they are restricted to a very thin interval located at the very base of the succession, ranging from centimetres to 1–2 m thick. Despite age dates tend to overlap with the underlying Oxfordian Heather and Hugin sandstones, biostratigraphic data suggest that Oxfordian deposits, attributable to the intra-Draupne Formation sandstones, existed on the Avaldsnes High. This is also supported by the distribution and age dates of the Heather and Hugin formations in Olsen et al. (2017), who described a Callovian-Oxfordian shoreline in this region.

5.3.3 | Kimmeridgian to Early Volgian flooding and establishment of a semi-restricted lagoon in the Augvald Graben

Parasequence 1 is mainly Kimmeridgian-Early Volgian in age (Figure 8a–c). The areal extent of this unit and the eventual terminations towards the northernmost and southernmost portion of the Augvald Graben (wells 16/2-19, 16/2-19A, 16/5-2S and 16/5-4), and towards the crest of the Avaldsnes High (wells 16/2-7A and 16/2-6), allows to reconstruct the trace of a restricted water mass in the Augvald Graben confined by local basement elevations along the crest of the Avaldsnes High (Figures 7a and 8a,b). This is interpreted as a low-energy lagoonal area along the eastern margin of the Haugaland High, based on the presence of fine-grained, upper shoreface deposits strongly bioturbated by *Macaronichnus segregatis* (FA-1) (Dashtgard et al., 2012). A higher energy setting is interpreted in the inner portions of the Augvald Graben, as evidenced from the basinward grain size increase in unit 1, typically recorded in restricted tidal systems such as lagoons and embayments (Figure 9a). Exposed basement elevations in the Avaldsnes High are interpreted as local features because they alternate with areas in which parasequence 1 is present (wells 16/2-16, 16/3-5, 16/3-8S and 16/3-7). Fan delta systems are interpreted based on the recognition of progradational and retrogradational fan delta lobe deposits (FA-6). The entry point of these systems is interpreted to be coincident with the position of the coarsest wells in the Haugaland High eastern

FIGURE 9 Palaeogeographical reconstructions of the Draupne Formation. (a) Kimmeridgian-Early Volgian: localized fault activity promoted the development of a lagoonal system in the Augvald Graben which favoured the deposition and preservation of fine-grained sediments and the general absence of cross-stratified deposits. A series of gravel spits and tidal inlets flanked the emerged portions of the Avaldsnes High at that time. (b) Early-Middle Volgian: increased tectonic activity promoted the structuration of a narrow tidal strait between the Avaldsnes High and the Geitungen Terrace. Strong tidal currents reworked the fan deltas and coastal regoliths which were mainly redeposited as tidal bars along the axis of the Augvald Graben. Tidal currents continued supplying sediments to the gravel spit systems in the Avaldsnes High. (c) Late Volgian/Ryazanian: Eustatic sea level rise promoted drowning of the clastic source areas and deposition of the Draupne Shale. Inversion of tectonic structures generated local erosion of preexisting sponge reefs and their redeposition in the form of spiculitic sediments. (d) Barremian: continued sea level rise ended up flooding the Haugaland High and promoting the deposition of the Asgard Formation at the same time that inversion progressed.

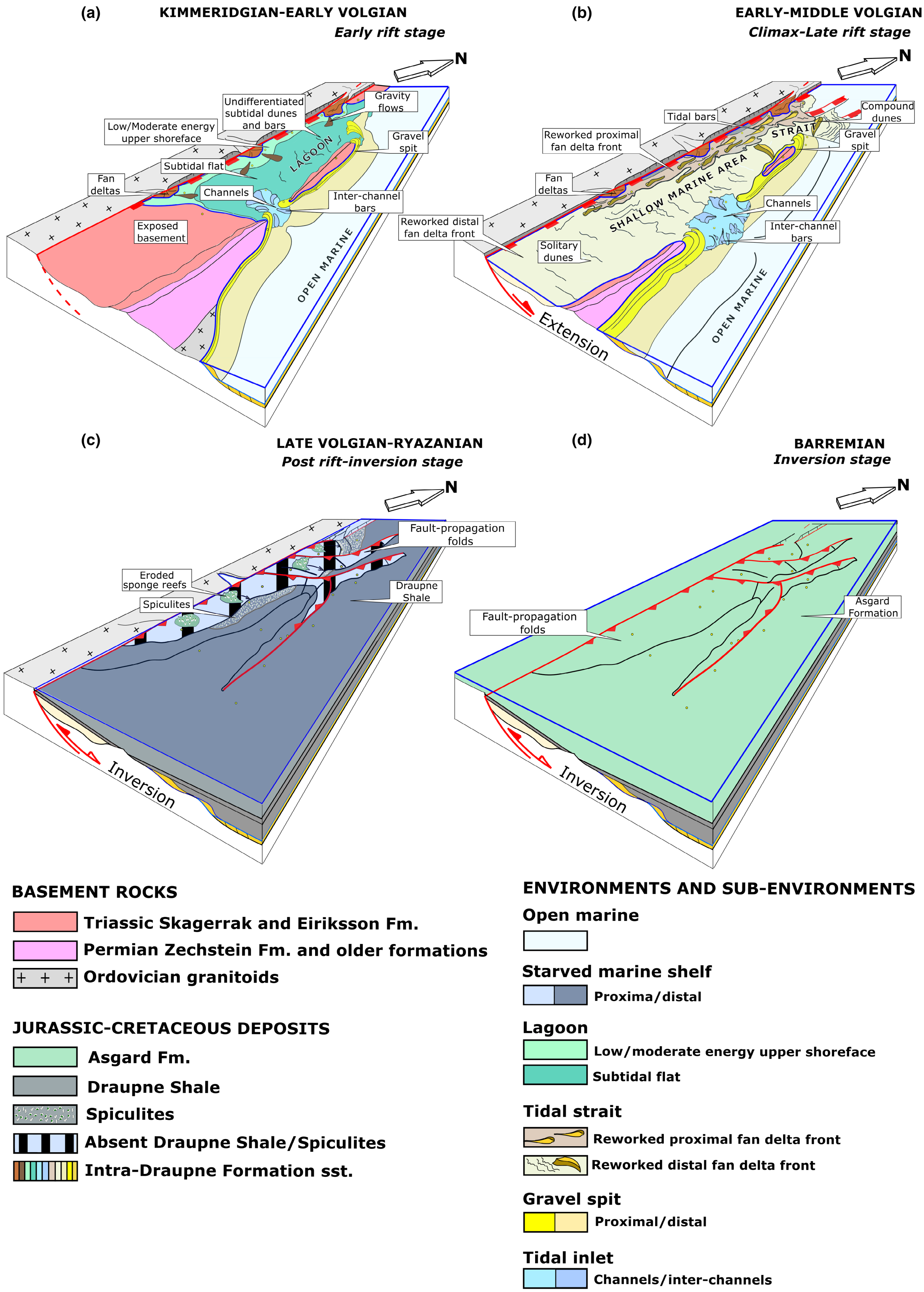
(a)
KIMMERIDGIAN-EARLY VOLGIAN
Early rift stage
N
Undifferentiated subtidal dunes and bars
Gravity flows
Low/Moderate energy upper shoreface
Gravel spit
Subtidal flat
LAGOON
Fan deltas
Channels
Inter-channel bars
Exposed basement
Reworked distal fan delta front
OPEN MARINE
(b)
EARLY-MIDDLE VOLGIAN
Climax-Late rift stage
N
Tidal bars
Compound dunes
Reworked proximal fan delta front
STRAIT
Gravel spit
Fan deltas
SHALLOW MARINE AREA
Channels
Inter-channel bars
Solitary dunes
Extension
OPEN MARINE
(c)
LATE VOLGIAN-RYAZANIAN
Post rift-inversion stage
N
Fault-propagation folds
Eroded sponge reefs
Draupne Shale
Spiculites
Inversion
(d)
BARREMIAN
Inversion stage
N
Asgard Formation
Fault-propagation folds
Inversion
BASEMENT ROCKS
Triassic Skagerrak and Eiriksson Fm.
Permian Zechstein Fm. and older formations
Ordovician granitoids
JURASSIC-CRETACEOUS DEPOSITS
Asgard Fm.
Draupne Shale
Spiculites
Absent Draupne Shale/Spiculites
Intra-Draupne Formation sst.
ENVIRONMENTS AND SUB-ENVIRONMENTS
Open marine
Starved marine shelf
Proxima/distal
Lagoon
Low/moderate energy upper shoreface
Subtidal flat
Tidal strait
Reworked proximal fan delta front
Reworked distal fan delta front
Gravel spit
Proximal/distal
Tidal inlet
Channels/inter-channels

margin, 16/5-3T2, 16/2-17S and 16/2-12 (Figure 9a). Gravel-rich sediments along the crest of the Avaldsnes High are interpreted to have been transported and deposited by SE-NW longshore and/or tidal currents, forming a series of gravel spits or barriers (Figures 5–7a and 9a). Channels through the gravel spits and between basement elevations, interpreted as tidal inlets (FA-3) (sensu Hayes & Fitzgerald, 2013), connected the lagoon with the open marine environment east of the crest of the Avaldsnes High, as recorded in the deposits of well 16/2-21 and the SW–NE palaeocurrent trends observed in wells 16/2-7, 16/3-5 and 16/3-4 (Figures 5 and 9a). These inlets are typical in systems with a moderate to high tidal range and explain the coarse-grained sandstones in the inner portions of the Augvald Graben and the presence of cross-stratified bedforms interbedded with muddy sandstones in well 16/2-15 (FA-2) (Figure 4b).

5.3.4 | Early to Middle Volgian fan delta front reworking and redeposition in a tidal strait

There is a significant change in basin configuration between the deposition of the Kimmeridgian-Early Volgian aged parasequence 1 and the Early-Middle Volgian deposits of parasequences 2–4. There is an absence of fine-grained facies in parasequences 2, 3 and 4. The well-sorted and coarser grain size, the predominance of NNE–SSW bidirectional cross-bedding and the *Skolithos* ichnofacies indicate deposition in a higher energy, shallow marine environment with strong axial circulation, in contrast to the lagoonal system of parasequence 1 (Figures 5–7b and 9b). Evidence for a pulse of strong tectonic activity during the transition from the Kimmeridgian-to-Early Volgian, is suggested by drastic fault-related thickness variations in parasequence 2, 3 and 4, in contrast to unit 1, in the hanging wall of the Main Boundary Fault, the Geitungen and Espevaer faults, and probably the Kvalen Graben Fault (Figure 8a–c). Together these faults created a 7.5 km wide and relatively deep, scoop-shaped trough, of tectonic origin, between well 16/2-16, in the northern Avaldsnes High, and well 16/2-19A, in the Geitungen Terrace (Figure 8c). This trough is interpreted as a tidal strait (Figure 9b) (Longhitano, 2011, 2013). The opening of the strait in Early Volgian times increased the energy regime in the basin, due to lateral restriction, and hence modified the type of depositional systems, from a semi-restricted lagoonal system in parasequence 1 to a higher energy tidal strait system in parasequences 2 to 4.

Based on the facies associations and palaeocurrent distribution in the Johan Sverdrup Field (Figures 5–7b) it is interpreted that the preexisting fan delta systems suffered of a strong degree of tidal reworking at that time. Given the NNE–SSW bidirectional palaeocurrents in the deposits on the eastern margin of the Haugaland High, oblique to the axis of the Augvald Graben (Figure 5), we suggest that fan delta fronts were predominantly reworked as tidal bars (Figure 9b) (Desjardins et al., 2012; Messina et al., 2014; Olariu et al., 2012). Basinwards, and in the inner portions of the Augvald Graben, where palaeocurrents are more parallel to the graben axis and the grain size is relatively finer, sediment could have been accumulated as tidal bars or solitary/compound dune fields (Figures 5 and 9b) (see Section 6). In the Avaldsnes High, the gravel spit system continued growing and accreting sediments during this time (Figure 9b). Similarly, the former tidal inlets kept active and promoting sediment exchange between the Augvald Graben and the eastern margin of the Avaldsnes High. Bedset scale palaeocurrent clusters showing opposite orientations indicate that individual and compound dunes/bars in the intra-Draupne Formation sandstones were likely generated during both ebb and flood periods (Figure 5). The dominance of northwards and southwards-directed palaeocurrents in the northern and southern Augvald Graben, respectively, and the co-dominance of both phases in between these areas, is interpreted to result from the variation in the dominant current speed and can be tentatively correlated with the strait-end and dune bedded-strait centre zones of modern and ancient tidal straits (Longhitano, 2013; Longhitano & Chiarella, 2020). Additionally, dip-meter data is steeper in wells 16/2-8 and 16/2-14, the dune bedded-strait centre zone, than at the fault tips, in wells 16/2-12 or 16/5-2S, the strait-end zone (Figure 5), which may indicate the existence of steeply dipping, high relief bedforms passing to gentler and smoother bedforms as the current speed decreases towards the strait-end zones (see Discussion section).

5.3.5 | Middle-to-Late Volgian/Ryazanian transgression and sediment starvation during a changing tectonic regime

The creation of accommodation started to exceed the rate of sedimentation during the deposition of parasequence 4. Despite that, a significant thickness increase of Unit 4 towards the hanging wall of the Geitungen Fault, rather than towards the Main Boundary Fault (Figure 8b,c), suggests that a slight rotation of the stress field might have taken place during this time interval, so that extension was mainly accommodated along the SW–NE oriented Geitungen and Espevaer faults, although this is somewhat speculative. As described in the Facies Analysis chapter, parasequence 4 is relatively finer than the underlying parasequences 2 and 3. This might indicate that this unit is a progradational parasequence formed during an overall retrogradational trend starting at this time. This process was accelerated during the local deposition of the early retrogradational interval and the widespread Condensed Section, which records a regional flooding of the area. The deposition of the Condensed Section took place during intra-Middle Volgian times throughout the majority of the basin (Figures 1c and 8a–c). However, some uncertain Early Volgian datings in well 16/2-13S of the Avaldsnes High eastern margin, and in well 16/2-19A of the Geitungen Terrace, indicate it might be slightly diachronous. This flooding is associated with an important backstepping of the feeder systems and, subsequent sediment starvation, as evidenced from the dark colour of the deposits and the high amount of nodules and belemnite fragments. Additionally, the thickness of the Condensed Section is relatively constant throughout the basin, indicating the exceedance of the rate of sediment supply over the rate of tectonic accommodation (Figure 8a–c). Biostratigraphic data suggest this started during the Middle Volgian at least, possibly during the Early Volgian, coevally with the deposition of the Draupne Formation black shales and spiculitic sandstones in the eastern margin of the Avaldsnes High and the Geitungen Terrace, where they attain a maximum thickness of 15 and 12 m, respectively (Figures 7c and 8a–c). The overlaying Draupne Shale deposits progressively onlapped onto the crest of the Avaldsnes High, the Augvald Graben and some portions of the Haugaland High eastern margin during the Late Volgian-Late Ryazanian (Figures 1c and 8a). The Draupne Shale shows some local and regional thickness variations that contrast with the rather constant thickness of the Condensed Section and do not correlate with the wedge geometries observed within the intra-Draupne Formation sandstones. As shown in the seismic lines (Figure 3), the correlation panels (Figure 8) and the facies map (Figure 7c), the Volgian-Late Ryazanian interval of the Draupne Shale thins and pinches-out towards the hanging wall of the Main Boundary Fault, the Geitungen Fault and the scoop-shaped depression in between, coincident with the position of some relatively broad anticline structures (Figures 3, 7c and 8). These structures mainly affected the upper Asgard Formation and are interpreted as propagation folds generated during an Early Cretaceous inversion phase (discussed in detail in the next section). The progressive onlap and pinchout of the Draupne Shale around these folds suggest that they may have been active during sedimentation; however, this is somewhat uncertain (see next section). The lack of preserved or in situ sponge reefs and the concentration of the spiculitic sediments around the anticlines suggests that the original reefs grew on top of these structures but were lately eroded, shedding fragments to the surrounding areas which were encased within the Draupne Formation black shales (Figures 7c and 9c).

5.3.6 | Early Cretaceous inversion of preexisting tectonic structures and fault-throw reconstruction

Deposition of the Asgard Formation mainly began during the Valanginian-Hauterivian period in the Geitungen Terrace, the southern portion of the Avaldsnes High and the Augvald Graben (Figures 1c and 8a–c), whereas in the rest of the field it is younger, especially at the top of the Haugaland High footwall, along its eastern margin and in the scoop-shaped depression at the northern Avaldsnes High, where it dates as mainly Barremian to locally Aptian in age (Figures 1c, 7d, 8a and 9d). The Asgard Formation is 3 to 35 m thick, attaining its maximum thickness in the Avaldsnes High eastern margin. The progressive thinning of the formation towards the main faults (Figure 8a–c), along with the identification of hanging wall anticline structures (Figure 3) is indicative of an inversion phase in the Johan Sverdrup Field. Inversion of pre-existing structures is much clearly recorded in the Barremian and younger intervals of the Asgard Formation, which are continuous throughout the whole basin and show a clear thinning towards the hanging wall of the Main Boundary Fault and Geitungen Fault (Figure 8a–c). The progressive thinning and disappearance of the Valanginian-Hauterivian Asgard Formation and the Late Volgian-Ryazanian Draupne Shale and associated spiculitic sandstones is less clear and more challenging to interpret (see Discussion section). Late Jurassic inversion in the Johan Sverdrup Field has further implications for fault scarp reconstructions. The thickness of the Asgard Formation at the footwall and hanging wall of the Main Boundary Fault is 3 and 7 m, respectively (Figure 8a). The similar thickness of the Barremian aged deposits on both sides of the Main Boundary Fault suggests that both occupied a similar structural level during sedimentation. The Asgard Formation is much thicker away from the influence of the Main Boundary Fault, showing a constant thickness of 25 to 35 m across the entire Johan Sverdrup Field. If thickness in these areas is considered to reflect the structural regional elevation (Cooper et al., 1989), then the Main Boundary Fault hanging wall must have experienced a 18–28 m of tectonic uplift, which suggests a Late Jurassic backstripped fault scarp of 22–32 m. Consequently, the catchment and drainage systems of the Haugaland High would have been highly incised and characterized by rather steep gradients during the deposition of the Intra-Draupne Formation sandstones.

6 | DISCUSSION

6.1 | From a semi-restricted lagoonal system to a higher energy tidal strait system

The extent of Unit 1 along with the interpreted facies and facies associations suggests the existence of a lagoonal system in the Augvald Graben during the Kimmeridgian-Early Volgian. Basinward increase in grain size is typically recorded in restricted tidal systems such as lagoons and embayments, where fine-grained sediments are located in supra tidal marshes and muddy inter-tidal flats passing seawards into coarser sediments in sand inter-tidal and subtidal portions of the system (Gao, 2019). As introduced, the source area for the Late Jurassic deposits was the Haugaland and Avaldsnes granitic basement, which was weathered into regolithic solids and then transported (Riber et al., 2015). Clay minerals are a common product in weathering soils resulting from the dissolution of feldspar-rich granitic rocks (Tardy et al., 1973; Yuan et al., 2019). While Unit 1 preserves fine-grained sandstones and muds, these should be expected in the overlying units too, based on the composition of the regoliths found on top of the structural highs (Riber et al., 2015). The triggering mechanism behind the general lack of fine-grained material and dominance of clean waters during the deposition of units 2, 3 and 4, is interpreted to be controlled by the opening of the shallow marine tidal strait in the Kimmeridgian-Early Volgian transition. Funnelling of water between topographic barriers, as in seaways or straits, enhances the strength of circulating current, facilitates the transport of coarse-grained particles and prevents deposition of fine-grained material (Longhitano, 2011, 2013; Longhitano & Chiarella, 2020). Deflection of fan delta fronts and reworking of pre-existing deposits is commonly observed in modern and ancient tide-dominated seaways and straits (Longhitano, 2011, 2013; Nakken et al., 2023; Rossi et al., 2017). Sediment feeder systems are reworked and redeposited along and/or oblique to the shoreline in the form of spits and a range of submarine bedforms. These bedforms classically fall into three main categories: compound tidal dunes/sand waves; sand sheets/sand banks and, tidal bars/sand ridges (Desjardins et al., 2012; Messina et al., 2014; Olariu et al., 2012). These are all characterized by cross-stratified deposits, some of them vertically stacked forming coarsening or fining upwards stratigraphic intervals separated by reactivation surfaces (Longhitano, 2018). Compound tidal dunes and sand sheets/sand banks tend to migrate forward, while tidal bars and sand ridges have a stronger lateral or oblique component respect to the main current (Messina et al., 2014; Olariu et al., 2012). It is challenging to differentiate them in subsurface, core-based datasets, compared with modern or outcrop examples. The interpreted tidal bars along the eastern margin of the Haugaland High accreted sediment at an oblique angle with respect to the interpreted palaeoflows, which mainly paralleled the axis of the Augvald Graben (Figures 4–7). The dominant bedform type in the inner portions of the Augvald graben is more uncertain; however, it is suggested that tidal bars and elongated bedforms might evolve into large dune and small dune fields as the tidal energy decreases close to the strait-end zones (Longhitano, 2018; Longhitano & Chiarella, 2020). Additionally, the dip angle of the palaeocurrent data is relatively low throughout most of the intra-Draupne Formation sandstones, 5°–15°, up to 20°–25° in wells 16/2-8 and 16/2-14 (Figure 5). These dip angles are generally low for dune cross-bedding and are more typically recorded for master and accretion surfaces in tidal bars and compound dunes (Longhitano, 2013; Olariu et al., 2012), indicating that the dip-meter dataset might be rather representing the higher-order surfaces. This can be observed in wells 16/2-8 and 16/2-14, where the steeper readings, between 15° and 25°, could reflect dune cross-bedding, and the gentler readings, 5° to 15°, could be related with master bedding surfaces. The lack of steeply dipping dip-meter data towards the interpreted strait-end zone could be related with the dominance of lower relief bedforms as a result of current speed decrease, or instead, readings related to master bedding surfaces. Unfortunately, the resolution of the FMI palaeocurrent data is not enough to tie the dip-meter readings to either the cross-beds or the reactivation surfaces identified in our stratigraphic logs of the intra-Draupne Formation sandstone.

6.2 | Comparison with previous intra-Draupne Formation models and interpretations in the Johan Sverdrup Field

Olsen et al. (2017) and Ottesen et al. (2022) are the main existing works focusing on the Johan Sverdrup Field. Both dealt with the facies description and interpretation of the intra-Draupne Formation sandstones. Sedimentary logs at 1:50 scale and correlation panels are mainly provided in Olsen et al. (2017), while palaeogeographical reconstructions are the main output of Ottesen et al. (2022). Both studies stated that they found difficulties recognizing internal surfaces of sequence stratigraphic significance, therefore hindering a detailed breakdown and correlation of the succession. Although we generally agree with the overall facies analysis in both studies, there are important novelties which are discussed in detail in the following sections.

6.2.1 | Correlation panels and palaeogeographical reconstructions of the intra-Draupne Formation sandstones

Correlation panels of the intra-Draupne Formation sandstones are available in Olsen et al. (2017) and consist of one section across the Augvald Graben. The palaeogeographical reconstructions of Olsen et al. (2017) suggest that Kimmeridgian sedimentation was limited to a narrow shoreface or spit located in the crest of the Avaldsnes High and its eastern margin. In Early-Middle Volgian times, the Avaldsnes region was completely transgressed and the Augvald Graben flooded, as a consequence of the Main Boundary Fault reactivation. The shoreline quickly retrograded westwards towards the Haugaland High eastern margin, where it occupied a relatively stable position above fair weather wave base, also influenced by long-shore and tidal currents which reworked the fan deltas and prevented the deposition of fine-grained particles. The same authors propose that most of the deposits at the crest of the Avaldsnes High and its eastern margin, corresponding to our parasequence 1, 2 and 3, were older and disconnected from the succession observed in the Augvald Graben and the eastern margin of the Haugaland High, and that parasequence 4 passes laterally to the Condensed Section and Draupne Shale deposits. As discussed in the correlations proposed in our study (Figure 8), there are no lateral facies change observed between the intra-Draupne Formation sandstones parasequences and the Draupne Shale or the Condensed Section, indicating they are not coeval, at least in the study area.

Our interpretation of the Early-Middle Volgian palaeogeography is more in line with the Early-Late Tithonian reconstruction of Ottesen et al. (2022) who emphasized: (1) the existence of a long-term barrier or shoal in the crest of the Avaldsnes High, and (2) the reworking of fan delta front deposits and regoliths in a high energy environment. Some important novelties lie in the palaeogeography of the Kimmeridgian period and the transition from our parasequence 1 and 2 at the Kimmeridgian-Early Volgian boundary. Ottesen et al. (2022) included the corresponding deposits of both parasequence into a single Late Kimmeridgian-Early Tithonian reconstruction, with coeval fine-grained muddy sandstones sedimentation in the eastern margin of the Haugaland High, strong fan-delta front reworking and migration of bidirectional coarse-grained bedforms. Our results suggest the two depositional parasequences bear significantly different characteristics. Ottesen et al. (2022) interpreted the bioturbated fine-grained sandstones of parasequence 1 as part of fan delta toe-sets deposited in a shelfal setting, with no further consideration of the absence of these deposits in the upper units and the upward grain size increase and abundance of cross-stratified deposits during the Early-Middle Volgian, although, a connection between the northern Augvald Graben and the eastern side of the Avaldsnes High seems to be suggested in their reconstructions, which could be potentially analogous to our tidal strait.

6.2.2 | Deposition of the Draupne Shale and Asgard Formation

Ottesen et al. (2022) suggest that deposition of spiculitic sandstones of the Draupne Shale in the Geitungen Terrace began in the Early Kimmeridgian, synchronous with the intra-Draupne Formation sandstones. The spiculitic deposits are the result of erosion and redeposition of siliceous sponge reefs, which were common in the Jurassic (Leinfelder, 2001), and proliferated during and after the drowning of the clastic source areas and the reduction of current strength. Our correlation panels suggest that spiculitic sandstones began to accumulate after the deposition of parasequence 4, in the Middle Volgian, mainly, once sediment supply and energy regime in the basin depleted. Consequently, we interpret that the Draupne Shale and the associated spiculitic facies are younger than the intra-Draupne Formation sandstones. Previous authors explain the progressive thinning of the Draupne Shale towards the West as a regional eastern tilting of the Avaldsnes High, mainly as a consequence of the syn-sedimentary tectonic activity of the Øygarden Fault Zone in the eastern margin of the Stord Basin (Fazlikhani et al., 2021). Our correlation panels suggest that inversion of the preexisting structures along with regional sea level rise is a plausible alternative or complement to explain the thickness variations and facies distribution of the Draupne Shale in the Johan Sverdrup Field. The interpreted onlap towards the hanging wall of the main faults could be an apparent feature resulting from post-depositional erosion associated with anticline growth and uplift during the Barremian inversion phase. However, similar inversion of pre-existing structures, affecting the Draupne Formation, and starting in the late Early Volgian and lasting until the Late Albian, was documented by Jackson and Larsen (2008) in the South Viking Graben, which supports the interpretation of an inversion phase starting in the Late Volgian-Ryazanian in our study area.

7 | CONCLUSIONS

In this study, a new sequence stratigraphic correlation constrains the evolution of the intra-Draupne Formation sandstones, the Draupne and Asgard formations in the Johan Sverdrup Field, southern Utsira High.

High-resolution logging allowed the identification of subtle grain size trends within a rather homogeneous coarse-grained shallow marine succession, which in turn led to the identification of multiple, previously undocumented sequence stratigraphic surfaces. This analysis detects four parasequences tied to the different tectonic events which affected the basin. We can conclude that:

1. Extensional tectonics controlled Late Jurassic depocenters and the deposition of the intra-Draupne Formation sandstones in the Johan Sverdrup Field.
2. Four parasequences along with seven facies and six facies' associations constitute the fundamental building blocks of the intra-Draupne Formation sandstones.
3. The basin configuration changed from a Kimmeridgian semi-restricted lagoonal system to a shallow tidal strait in the Early Volgian and, finally, to a sediment-starved marine shelf in the Middle Volgian-Late Volgian transition.
4. Fan delta fronts along the eastern margin of the Haugaland High were mainly reworked as tidal bars, whereas the sediments along the Avaldsnes High accumulated forming a gravel spit system, locally dissected by tidal inlets and small basement elevations.
5. A Late Volgian-Barremian inversion phase occurs affecting the Draupne Shale and Asgard Formation, in agreement with previous studies in the south Viking Graben, and involving the Johan Sverdrup Field.
6. A 22 to 32 m high Late Jurassic fault scarp is interpreted after restoring the inversion of the Main Boundary Fault, which would have favoured steep gradients and the formation of fan deltas and coarse-grained sediment delivery to the Augvald Graben.

These results increase the understanding of the depositional environment of the intra-Draupne Formation sandstones and help identifying coarse-grained shallow marine subsurface deposits which accumulated around transgressed structural highs, epeiric seas and continental margins. They also bear useful implications for assessing the energetic potential of regions nearby the Johan Sverdrup Field, placing any potential future reservoir within a Late Jurassic sequence stratigraphic framework for the Norwegian North Sea, around the southern Utsira High.

ACKNOWLEDGEMENTS

We gratefully acknowledge the Norwegian Research Council (grant agreement 295208) and the companies Aker BP, Lundin, Equinor and Spirit Energy for sponsoring the Suprabasins project. Special thanks are given to the former exploration and production departments of Lundin Energy Norway (Aker BP now) for fruitful discussions during the first author's internship at the company. Editor-in-chief Atle Rotevatn and reviewers Ron Steel, Domenico Chiarella and Sergio Longhitano are gratefully acknowledged for their constructive reviews and fruitful comments which have improved the quality of this manuscript.

CONFLICT OF INTEREST STATEMENT

There is no conflict of interest.

DATA AVAILABILITY STATEMENT

The data that support the findings of this study are available on request from the corresponding author. The data are not publicly available due to privacy or ethical restrictions.

ORCID

Josep M. Puig López https://orcid.org/0000-0002-4308-3454
Miquel Poyatos-Moré https://orcid.org/0000-0001-7813-8868

REFERENCES

Baniak, G. M., Gingras, M. K., Burns, B. A., & Pemberton, G. (2014). An example of a highly bioturbated, storm-influenced shoreface deposit: Upper Jurassic Ula Formation, Norwegian North Sea. *Sedimentology*, *61*(5), 1261–1285. https://doi.org/10.1111/sed.12100

Biddle, K. T., & Rudolph, K. W. (1988). Early Tertiary structural inversion in the Stord Basin, Norwegian North Sea. *Journal of the Geological Society, London*, *145*, 603–611. https://doi.org/10.1144/gsjgs.145.4.0603

Chiarella, D., Longhitano, S. G., Mosdell, W., & Tellesca, D. (2020). Sedimentology and facies analysis of ancient sand ridges: Jurassic Rogn Formation, Trøndelag Platform, offshore Norway. *Marine and Petroleum Geology*, *112*, 104082. https://doi.org/10.1016/j.marpetgeo.2019.104082

Cooper, M. A., Williams, G. D., de Graciansky, P. C., Murphy, R. W., Needham, T., de Paor, D., Stoneley, R., Todd, S. P., Turner, J. P., & Ziegler, P. A. (1989). Inversion tectonics—A discussion. *Geological Society, London, Special Publications*, *44*, 335–347. https://doi.org/10.1144/GSL.SP.1989.044.01.18

Copestake, P., Sims, A. P., Crittenden, S., Hamer, G. P., Ineson, J. R., Rose, P. T., & Tringham, M. E. (2003). Lower Cretaceous. In D. Evans, C. Graham, A. Armour, & P. Bathurst (Eds.), *The Millenium Atlas: Petroleum geology of the central and northern North Sea* (pp. 191–211). The Geological Society of London.

Cornford, C. (1998). Source rocks and hydrocarbons of the North Sea. In K. W. Glennie (Ed.), *Petroleum geology of the North Sea: Basic concepts and recent advances* (4th ed., pp. 376–462). Blackwell Science Ltd. https://doi.org/10.1002/9781444313413.ch11

Dashtgard, S. E., MacEachern, J. A., Frey, S. E., & Gingras, M. K. (2012). Tidal effects on the shoreface: Towards a conceptual framework. *Sedimentary Geology*, *279*, 42–61. https://doi.org/10.1016/j.sedgeo.2010.09.006

Desjardins, P. R., Buatois, L., & Mángano, M. G. (2012). Tidal flats and subtidal sand bodies. In D. Knaust & R. Bromley (Eds.), *Developments in sedimentology: Trace fossils as indicators of sedimentary environments* (Vol. *64*, pp. 529–561). Elsevier. https://doi.org/10.1016/B978-0-444-53813-0.00018-6

Dreyer, T., Whitaker, M., Dexter, J., Flesche, H., & Larsen, E. (2005). From spit system to tide-dominated delta: Integrated reservoir model of the Upper Jurassic Sognefjord Formation on the Troll West Field. In A. G. Doré & B. A. Vining (Eds.), *Petroleum geology: North-West Europe and global perspectives—Proceedings of the 6th Petroleum Geology Conference* (Vol. *6*, pp. 423–448). Geological Society. https://doi.org/10.1144/0060423

Fazlikhani, H., Aagotnes, S. S., Refvem, M. A., Hamilton-Wrigth, J., Bell, R. E., Fossen, H., Gawthorpe, R. L., Jackson, C. A.-L., & Rotevatn, A. (2021). Strain migration during multiphase extension, Stord Basin, northern North Sea rift. *Basin Research*, *33*(2), 1474–1496. https://doi.org/10.1111/bre.12522

Gao, S. (2019). Geomorphology and sedimentology of tidal flats. In G. M. E. Perillo, E. Wolanski, D. R. Cahoon, & C. S. Hopkinson (Eds.), *Coastal wetlands: An integrated ecosystem approach* (pp. 359–381). Elsevier. https://doi.org/10.1016/B978-0-444-63893-9.00010-1

Gautier, D. L. (2005). Kimmeridgian shales total petroleum system of the North Sea Graben Province. *US Geological Survey Bulletin*, *2204C*, 1–24.

Hart, B. S., & Plint, A. G. (1995). Gravelly shoreface and beachface deposits. In A. G. Plint (Ed.), *Sedimentary facies analysis: A tribute to the research and teaching of Harold G. Reading* (Vol. *22*, pp.75-99). The International Association of Sedimentologists. https://doi.org/10.1002/9781444304091.ch4

Hayes, M. O., & Fitzgerald, D. M. (2013). Origin, evolution and classification of tidal inlets. *Journal of Coastal Research*, *69*, 14–33. https://doi.org/10.2112/SI_69_3

Henstra, G. A., Cullen, T. M., Gawthorpe, R. L., Munoz-Barrera, J. M., Muravchik, M., & Rotevatn, A. (2023). The evolution of catchment-depositional system relationships on the dip slopes of intra-rift basement highs: An example from the Frøya High, Mid-Norwegian rifted margin. *Basin Research*, *35*(4), 1259–1287. https://doi.org/10.1111/bre.12753

Howell, J. A., Flint, S. S., & Hunt, C. (1996). Sedimentological aspects of the Humber Group (Upper Jurassic) of the South Central Graben, UK North Sea. *Sedimentology*, *43*, 89–114. https://doi.org/10.1111/j.1365-3091.1996.tb01462.x

Jackson, C. A.-L., & Larsen, E. (2008). Temporal constraints on basin inversion provided by 3D seismic and well data: A case study from the South Viking Graben, offshore Norway. *Basin Research*, *20*, 397–417. https://doi.org/10.1111/j.1365-2117.2008.00359.x

Jackson, C. A.-L., Kane, K., Larsen, E., Evrard, E., Elliot, G., & Gawthorpe, R. (2012). Variability in syn-rift structural style associated with a mobile substrate and implications for trap definition and reservoir distribution in extensional basins: A subsurface case study from the South Viking Graben, Offshore Norway. *AAPG Search and Discovery*, Article 10423.

Jackson, C. A.-L., Kane, K. E., & Larsen, E. (2010). Structural evolution of minibasins on the Utsira High, northern North Sea; implications for Jurassic sediment dispersal and reservoir distribution. *Petroleum Geoscience*, *16*, 105–120. https://doi.org/10.1144/1354-079309-011

Johnson, H. D., Mackay, T. A., & Stewart, D. J. (1986). The Fulmar Oil-field (Central North Sea): Geological aspects of its discovery, appraisal and development. *Marine and Petroleum Geology*, *3*(2), 99–125. https://doi.org/10.1016/0264-8172(86)90023-1

Jørstad, A. (2012). Johan Sverdrup—Offshore Norway: The story behind the Giant Sverdrup discovery. AAPG Search and Discovery #20177.

Leinfelder, R. R. (2001). Jurassic reef ecosystems. In G. D. Stanley, Jr. (Ed.), *The history and sedimentology of ancient reef systems* (pp. 251–309). Kluwer Academic/Plenum Publishers.

Leithold, E. L., & Bourgeois, J. (1984). Characteristics of coarse-grained sequences deposited in nearshore, wave-dominated environments-examples from the Miocene of south-west Oregon. *Sedimentology*, *31*(6), 749–775. https://doi.org/10.1111/j.1365-3091.1984.tb00884.x

Longhitano, S. (2011). The record of tidal cycles in mixed silici–bioclastic deposits: Examples from small Plio–Pleistocene peripheral basins of the microtidal Central Mediterranean Sea. *Sedimentology*, *58*(3), 691–719. https://doi.org/10.1111/j.1365-3091.2010.01179.x

Longhitano, S. (2013). A facies-based depositional model for ancient and modern, tectonically–confined tidal straits. *Terra Nova*, *25*(6), 446–452. https://doi.org/10.1111/ter.12055

Longhitano, S. (2018). Between Scylla and Charybdis (part 2): The sedimentary dynamics of the ancient, Early Pleistocene Messina Strait (central Mediterranean) based on its modern analogue. *Earth-Science Reviews*, *179*, 248–286. https://doi.org/10.1016/j.earscirev.2018.01.017

Longhitano, S., & Chiarella, D. (2020). Tidal straits: Basic criteria for recognizing ancient systems from the rock record. In N. Scarselli, J. Adam, D. Chiarella, D.G. Roberts, & A. W. Bally (Eds.), *Regional geology and tectonics: Principles of geologic analysis* (Vol. *1*, pp. 365–415). Elsevier. https://doi.org/10.1016/B978-0-444-64134-2.00014-6

Longhitano, S., Mellere, D., Steel, R. J., & Ainsworth, R. B. (2012). Tidal depositional systems in the rock record: A review and new insights. *Sedimentary Geology*, *279*, 2–22. https://doi.org/10.1016/j.sedgeo.2012.03.024

MacEachern, J. A., & Hobbs, T. W. (2004). The ichnological expression of marine and marginal marine conglomerates and conglomeratic intervals, Cretaceous Western Interior Seaway, Alberta and northeastern British Columbia. *Bulletin of Canadian Petroleum Geology*, *52*(1), 77–104. https://doi.org/10.2113/52.1.77

MacEachern, J. A., Zaitlin, B. A., & Pemberton, S. G. (1998). High-resolution sequence stratigraphy of early transgressive deposits, Viking formation, Joffre Field, Alberta, Canada. *AAPG Bulletin*, *82*(5A), 729–756. https://doi.org/10.1306/1D9BC5E3-172D-11D7-8645000102C1865D

Mahmic, O., Dypvik, H., & Hammer, E. (2018). Diagenetic influence on reservoir quality evolution, examples from Triassic conglomerates/arenites in the Edvard Grieg field, Norwegian North Sea. *Marine and Petroleum Geology*, *93*, 247–271. https://doi.org/10.1016/j.marpetgeo.2018.03.006

Messina, C., Nemec, W., Martinius, A. W., & Elfenbein, C. (2014). The Garn Formation (Bajocian-Bathonian) in the Kristin Field, Halten Terrace: Its origin, facies architecture and primary heterogeneity model. In A. W. Martinius, R. Ravnås, J. A. Howell, R. J. Steel, & J. P. Wonham (Eds.), *From depositional systems to sedimentary successions on the Norwegian Continental Margin* (Vol. *46*, pp. 513–550). International Association of Sedimentologists. https://doi.org/10.1002/9781118920435.ch18

Nakken, L., Chiarella, D., & Jackson, A.-L. C. (2023). Late Jurassic rift physiography of the Froan Basin and Frøya High, offshore Mid-Norway: Development of a syn-rift shallow marine system. *Basin Research*, *35*(5), 1908–1932. https://doi.org/10.1111/bre.12785

Nemec, W., & Steel, R. J. (1984). Alluvial and coastal conglomerates: Their significant features and some comments on gravelly mass-flow deposits. In E. H. Koster, & R. J. Steel (Eds.), *Sedimentology of gravels and conglomerates* (Vol. *10*, pp. 1–31). Canadian Society of Petroleum Geologists.

Nøttvedt, A., Berge, A. M., Dawers, N. H., Færseth, R. B., Häger, K. O., Mangerud, G., & Puigdefabregas, C. (2000). Syn-rift evolution and resulting play models in the Snorre-H area, northern North Sea. In A. Nøttvedt (Ed.), *Dynamics of the Norwegian Margin* (Vol. *167*, pp. 179–218). Geological Society, Special Publications. https://doi.org/10.1144/GSL.SP.2000.167.01.08

Olariu, C., Steel, R. J., Dalrymple, R. W., & Gingras, M. K. (2012). Tidal dunes versus tidal bars: The sedimentological and architectural characteristics of compound dunes in a tidal seaway, the lower Baronia Sandstone (Lower Eocene), Ager Basin, Spain. *Sedimentary Geology*, *279*, 134–155. https://doi.org/10.1016/j.sedgeo.2012.07.018

Olsen, H., Briedis, N. A., & Renshaw, D. (2017). Sedimentological analysis and reservoir characterization of a multi-darcy, billion barrel oil field—The Upper Jurassic shallow marine sandstones of the Johan Sverdrup Field, North Sea, Norway. *Marine and Petroleum Geology*, *84*, 102–134. https://doi.org/10.1016/j.marpetgeo.2017.03.029

Ottesen, S., Selvikvåg, B., Scott, A. S. J., Meneguolo, R., Cullum, A., Amilia-Cabeza, A., Vigorito, M., Helsem, A., & Martinsen, O. J. (2022). Geology of the Johan Sverdrup Field: A giant oil discovery and development project in a mature Norwegian North Sea basin. *AAPG Bulletin*, *106*(4), 897–936. https://doi.org/10.1306/11042120037

Partington, M. A., Mitchener, B. C., Milton, N. J., & Fraser, A. J. (1993). Genetic sequence stratigraphy for the North Sea Late Jurassic and Early Cretaceous: distribution and prediction of Kimmeridgian-Late Ryazanian reservoirs in the North Sea and adjacent areas. In J. R. Parker (Ed.), *Petroleum geology of northwest Europe: Proceedings of the 4th Conference. Petroleum Geology Conference Series* (Vol. *4*, pp. 347–370). Geological Society. https://doi.org/10.1144/0040347

Phillips, T. B., Fazlikhani, H., Gawthorpe, R. L., Fossen, H., Jackson, C. A. L., Bell, R. E., Faleide, J. I., & Rotevatn, A. (2019). The influence of structural inheritance and multiphase extension on rift development, the Northern North Sea. *Tectonics*, *38*(12), 4099–4126. https://doi.org/10.1029/2019TC005756

Ravnås, R., & Steel, R. J. (1998). Architecture of marine rift-basin successions. *AAPG Bulletin*, *82*(1), 110–146. https://doi.org/10.1306/1D9BC3A9-172D-11D7-8645000102C1865D

Riber, L., Dypvik, H., & Sørlie, R. (2015). Altered basement rocks on the Utsira High and its surroundings, Norwegian North Sea. *Norwegian Journal of Geology*, *95*(1), 57–89. https://doi.org/10.17850/njg95-1-04

Riber, L., Dypvik, H., Sørlie, R., Naqvi, S. A. A. E. M., Stangvik, K., Oberhardt, N., & Schroeder, P. A. (2017). Comparison of deeply buried paleoregolith profiles, Norwegian North Sea, with outcrops from southern Sweden and Georgia, USA—Implications for petroleum exploration. *Palaeogeography, Palaeoclimatology, Palaeoecology*, *471*, 82–95. https://doi.org/10.1016/j.palaeo.2017.01.043

Rønnevik, H. C., Jørstad, A., & Lie, J. E. (2017). The discovery process behind the giant Johan Sverdrup Field. In R. K. Merill & C. A. Sternbach (Eds.), *Giant fields of the decade 2000–2010: AAPG Memoir* (Vol. *113*, pp. 195–220). The American Association of Petroleum Geologists. https://doi.org/10.1306/13572008M1133687

Rossi, V. M., Longhitano, S. G., Mellere, D., Dalrymple, R. W., Steel, R. J., Chiarella, D., & Olariu, C. (2017). Interplay of tidal and fluvial processes in an early Pleistocene, deltafed, strait margin (Calabria, Southern Italy). *Marine and Petroleum Geology*, *87*, 14–30. https://doi.org/10.1016/j.marpetgeo.2017.02.021

Scott, A. J., & Ottesen, S. (2018). Tectono-stratigraphic development of the Upper Jurassic in the Johan Sverdrup area. In C. C. Turner & B. T. Cronin (Eds.), *Rift-related coarse-grained submarine fan reservoirs; the Brae Play, South Viking Graben, North Sea: AAPG Memoir* (Vol. *115*, pp. 445–452). The American Association of Petroleum Geologists. https://doi.org/10.1306/13652190M1153815

Serck, C. S., Braathen, A., Hassaan, M., Faleide, J. I., Riber, L., Messager, G., & Midtkandal, I. (2022). From metamorphic core complex to crustal scale rollover: Post-Caledonian tectonic development of the Utsira High, North Sea. *Tectonophysics*, *836*, 229416. https://doi.org/10.1016/j.tecto.2022.229416

Tardy, Y., Bocquier, G., Paquet, H., & Millot, G. (1973). Formation of clay from granite and its distribution in relation to climate and topography. *Geoderma*, *10*, 271–284. https://doi.org/10.1016/0016-7061(73)90002-5

Thomas, D. W., & Coward, M. P. (1996). Mesozoic regional tectonics and South Viking Graben formation: Evidence for localized thin-skinned detachments during rift development and inversion. *Marine and Petroleum Geology*, *13*(2), 149–177. https://doi.org/10.1016/0264-8172(95)00034-8

Tillmans, F., Gawthorpe, R. L., Jackson, C. A.-L., & Rotevatn, A. (2021). Syn-rift sediment gravity flow deposition on a Late Jurassic fault-terraced slope, northern North Sea. *Basin Research*, *33*, 1844–1879. https://doi.org/10.1111/bre.12538

Underhill, J. R., & Partington, M. A. (1993). Jurassic thermal doming and deflation in the North Sea: Implications of the sequence stratigraphic evidence. In *Petroleum geology of Northwest Europe: Proceedings of the 4th Conference. Petroleum Geology Conference Proceedings* (Vol. *4*, pp. 337–345). The Geological Society of London. https://doi.org/10.1144/0040337

Van Wagoner, J. C., Posamentier, H. W., Mitchum, R. M., Vail, P. R., Sarg, J. F., Loutit, T. S., & Hardenbol, J. (1988). An overview of sequence stratigraphy and key definitions. In C. K. Wilgus, B. S. Hastings, C. G. S. C. Kendall, H. W. Posamentier, C. A. Ross, & J. C. Van Wagoner (Eds.), *Sea level* *changes—An integrated approach* (Vol. *42*, pp. 39–45). SEPM Special Publication.

Yuan, G., Cao, Y., Schulz, H.-M., Hao, F., Gluyas, J., Liu, K., Yang, T., Wang, Y., Xi, K., & Li, F. (2019). A review of feldspar alteration and its geological significance in sedimentary basins: From shallow aquifers to deep hydrocarbon reservoirs. *Earth-Science Reviews*, *191*, 114–140. https://doi.org/10.1016/j.earscirev.2019.02.004

Zanella, E., & Coward, M. P. (2003). Structural framework. In D. Evans, C. Graham, A. Armour, & P. Bathurst (Eds.), *The millennium atlas: Petroleum geology of the central and northern North Sea* (pp. 45–59). London: Geological Society.

How to cite this article: Puig López, J. M., Poyatos-Moré, M., & Howell, J. (2023). Facies analysis and sequence stratigraphy of shallow marine, coarse-grained siliciclastic deposits in the southern Utsira High: The Late Jurassic intra-Draupne Formation sandstones in the Johan Sverdrup Field (Norwegian North Sea). *Basin Research*, *00*, 1–29. https://doi.org/10.1111/bre.12833